Dear Editor,

Thank you to you and the reviewers for your valuable comments regarding our study. Our responses below and the improvements that we have made to the manuscript have now thoroughly addressed the remaining concerns of the reviewers. Specifically we have: 1) expanded the methods section to detail our treatment of the data and our calculations of BC mass transport, 2) removed more speculative aspects of the study (including the examination of back trajectories), 3) included greater description of the limitations of our data and the conclusions that we draw from it, and 4) ensured that the grammar and structure are of suitable quality for ACP. In all, these changes have helped to greatly improved our manuscript which we feel is now suitable for publication in ACP.

Thank you for your continued consideration,

Shradda Dhungel*

*shradda@virginia.edu

Reviewer #1

This is my second review of this paper. In respect to the first submission, the authors added some new elaborations/analyses and accepted some of my previous indications. The paper is improved from the original submission (as an instance the authors improved the motivation of the study and the manuscript organization) but more work is still necessary before it can be considered suitable for publications by ACP. Indeed, the paper still suffers of major deficiencies (both technical and scientific). It still appears somewhat confused and still difficult to follow. Besides the presentation of O3 and BC measurements at a new Himalayan location, no new information in respect to previous similar works have been provided (the main outcome of this paper is that the valley represent a "channel" for pollution to be transported at high altitudes). However, as I reported in my previous review, in the Himalaya region a need for measurements and scientific evidences still is needed, and the observations from KGV can provide useful information for (i) confirm the role of Himalaya valley as "preferred" way for the anthropogenic pollution to be transported up to high Himalaya, (ii) support the hypothesis that pollution from IGP and Himalaya foothills can be transported across mountain ridge to Tibetan Plateau or vented to the free troposphere, (iii) assess the contribution of open fires (or other emissions) to the occurrence of the ABC in South Asia/Himalayas region.

We thank the reviewer for his/her continued feedback on our manuscript. The main objective of this study is to present and describe new observational evidence of pollution transport from the Indo-Gangetic Plan through Himalayan mountain valleys to the higher Himalaya and Tibetan Plateau. We have clarified this main objective in the text and also clearly stated that our assessment of BC flux is preliminary and that future studies should seek to quantify flux and pollutant sources with greater depth and rigor. We have also removed any assessment of pollutant source regions as performed with back trajectories. We have also substantially reorganized the manuscript (particularly regarding the methods and results/discussion

sections). Below can be found our responses to specific comments made by reviewer #1, all of which have helped to greatly improve our manuscript.

From a technical point of view, the paper need a strong language revisions and the quality of some figures must be improved.
We have made a thorough, global review of the language for grammar and terminology and leave this technical aspect at the discretion of the editor. While we could not be certain to what specifically the reviewer was referring regarding figure quality, we have made several improvements to improve clarity and readability (see Figures 2 and 3).

For these reasons, I cannot recommend publication but reconsideration after major revisions.

MAJOR POINTS
In respect to my previous review you mentioned that "winter" was not considered in your paper because is "not relevant". Please, better argument this point: January and February are not winter months?
In the methods section, we define each season that we consider based on wet or dry season. The seasons are thus defined a pre-monsoon, monsoon and post-monsoon season. Winter months fall within the post-monsoon season.

Line 273: as already reported in my previous review, this is not true. The seasonal cycles ARE DIFFERENT between IGP and Himalaya foothills and Himalayas. Your BC peak is in pre-monsoon. While over the plains or foothills the peak is during winter (see also Putero et al., ACP, 2015 same special issue). The seasonal cycles are different not similar.
We have changed the text to more accurately reflect the differences in timing. The added text now reads "The post-monsoon timing of peak BC concentrations observed in previous studies performed in the IGP and Himalayan foothills (see e.g., Tripathi et al, 2005; 2007; Ramchandran et al., 2007; Putero et al, 2015) differs from our observations in the KGV, where we see heightened BC during the pre-monsoon season (Fig. 5). These findings are generally in agreement with other high altitude observations. For example, the Nepal Climate Observatory-Pyramid (NCO-P) station at the 5079 m asl in the Himalaya has also shown high seasonal differences for BC and O_3 between pre-monsoon (0.444 (±0.443) μg BC m^{-3}; 61 (±9) ppbv O_3) and monsoon (0.064 (±0.101) μg m^{-3}; 39 (±10) ppbv O_3) (Cristofanelli et al., 2010, Marinoni et al., 2013) (Table 2). Our results therefore indicate a lagged peak in BC and O_3 within the KGV and presumably other deep Himalayan valleys, as compared to sites within the IGP.".

Line 347-366: this discussion is out of the scope of the paper. Please remove.
We have removed this text.

Line 430: to provide a more robust assessment about the degree of mixing within the valley you should calculate the gradient of potential temperature between the two AWS...
We have created a plot of potential temperature to further support our argument. See Supplementary figure 2.

"Because….estimate". On which basis can you affirm that BC can be vented above 800 m agl.

Provide references.
We have now provided photographic evidence that the higher elevation JSM_2 was within the polluted layer (Supplementary Figure 1).

Section 3.4: you should better discuss the different relationship between BC and O3 for the different class of events, not only limiting to describe the observed behavior but also speculating about the reasons leading to the different co-variabilities. As an instance, why during the Pattern A no O3 enhancement is observed? On the other side for Pattern B the O3 is highest when BC is low. A mixed situations occur for pattern C. Please comment and provide explanations. Figure 8: please in the caption provide explanation for the dotted lines and blue/orange dots.
We prefer not to speculate about the reasons leading to different patterns as this would require a more robust analysis than is pursued in the present study. We have added a brief statement to indicate some of the factors that might contribute to these differences: "Different atmospheric lifetimes, chemical reactivity, source location, and sinks of BC and O_3 all may contribute to these differences in BC and O_3 concentrations detected in the valley." We have also improved the figure caption to indicate what the dashed lines and blue and orange dots represent.

The Conclusion Section looks like a simple summary/highlights of the evidences reported long the paper.

Once again: you should discuss the fact that only 2.5 years of observations are available. Thus you are not able to discuss and assess interannual variability of frequency and magnitude of observed pollution transport.
A conclusion section should indeed serve as a summary of the paper. We have modified the conclusion section and included mention of the limitations regarding interannual variability as highlighted by the reviewer.

TECHNICAL/SPECIFIC/LANGUAGE POINTS

Abstract-line 28: please revise this sentence ("particulary during preceeding the monsoon" replace with "pre-monsoon")
We have made the recommended change.

Line 182, please replace "climatologically important pollutants" with "essential climate variables (ECVs)"
We rewrote this phrase to read "two important SLCPs".

Line 192: I'm sorry but the valley orientation description is still obscure to me. What do you mean with "The valley is oriented southeasterly to northwesterly"? Maybe "The valley is oriented from SE to NW"? The same for the following sentences…
We clarified the text to read: "The general orientation of the valley is from SW (the mouth of the valley) to NE (the head of the valley) (Fig. 1)."

Figure 2: please for each site provide the start-end date of the available observations.

We have added the start and end dates of data availability.

Move Table 1 Supplementary to the main manuscript (section 2.1).
We have now moved Supplementary Table 1 to the main text.

Line 208: Again, more details about QA/QC should be reported. How the O3 sampling is executed? Do you use anti-particulate filters at the inlet lines (which type of filters?). By which frequency the instrument is calibrated? Against which standard? How the inlet line is made? Did you calculate the measurement uncertainty?
We have included greater detail about our pollutant sampling. The added text now reads: "The atmospheric observatory at Jomsom (JSM_STA) is equipped with instruments to measure BC, O_3, and meteorology (Figure 2). The observatory is located on the southeast corner of a plateau jutting out from an east-facing slope about 100 m above the valley floor and with no major obstructions either up or down the valley. Equivalent black carbon (hereafter referred to as BC) was measured with a Thermo Multiangle Absorption photometer (MAAP), model 5012 that uses a multi-angle photometer to analyze the modification of radiation fields – as caused by deposited particles that entered through a straight, vertical inlet line – in the forward and back hemisphere of a glass-fiber filter (GF-10). MAAP was operated at a flow rate of 20 L min^{-1}, measuring BC at 1-minute frequency. We note that Hyvärinen (2013) illustrates the artifact in MAAP measurements in environments with high aerosol loading with an underestimation of concentration above 9 µg m^{-3}. Since the median monthly concentrations for the duration of the measurement were less than 1µg m^{-3} and 90th percentile below 2 µg m^{-3} (and therefore below this threshold), MAAP corrections were not applied. O_3 was measured with a 2B Tech model 205 via the attenuation of ultraviolet light at 254 nm passing through a 15 cm long absorption cell fitted with quartz windows. The instrument was operated at a flow rate of 1.8 L min^{-1}. For instrument calibration, the BC instrument performed an automatic span and zero checks every 24 hours while zero checks on the O_3 instrument were performed every 7 days. Wind speed and direction were measured by an automated weather station installed on a ridge 900 m (JSM_2) above the sampling site for BC and O_3.".

Line 259: is not suppressed but reduced
We have made the recommended change.

Line 283: replace "seasonable" with "seasonal"
We have made the recommended change.

Line 296: please add formula to better explain you calculations. I'm still convinced that showing concentration (for BC) and mixing ratio (for O3) will provide more useful info for the audience.
Done, we added the formula for normalization in section 2.2 Data summary.

Line 319: use subscript for "3"
We have made the recommended change.

Line 319. "non-combustion sources": please explain more explicitly
It now reads, "or its precursors from non-combustion sources like stratospheric ozone and biogenic hydrocarbons from vegetation."

Line 329: something is missing in this sentence. "… are at minimum in the KGC, thus supporting the contribution of regional/long-range transport".
We have corrected this sentence.

Line 334: "in each seasons". Do you mean the single months showed by Figure 5? In the case, please, replace "pre-monsoon" with "Apr. 2013" and so on…The quality of Figure 2 is poor. Especially for post-monsoon is really difficult to read the wind roses. Please, zoom by decreasing the upper range of radius…
We have added the months that correspond with each season. However, it was unclear to us what specifically the reviewer meant by "poor quality" of Figure 2. We have modified the Figure 2 to ease its readability and believe that the figure adequately conveys its intended information. Small text at the bottom of the image is simply the result of taking image from Google Earth. As for the wind roses in Figure 5 now Figure 3, we wish to maintain consistent axes for all wind roses in order to allow comparison across time steps. We leave it to the editor to decide.

Line 392: Figure 4 appears after Figure 5 and 6 (section 3.2, 3.3). Please check and re-number figures where appropriate. Once again. Figure 4 is not useful for the paper. Each feature that you describe here can be (more easily) find looking at Figure 5 and 6. I suggest to move Figure 4 in the supplementary materials just to provide an overview of data.
We have ensured that figure numbers are consistent and ordered as they occur within the text.

Line 366: replace "one hour" with "1 hour"
We have made the recommended change.

Line 403: this is not true looking at Figure 5 where only 1 peak can be seen in late afternoon.
We have now clarified that this statement was in reference to BC concentration. The revised text now reads: "Distinct morning and afternoon peaks in BC concentration are seen in the post-monsoon season when the up-valley wind speeds are relatively weaker than in pre-monsoon season (Fig. 4 and 6)."

Line 406: replace "relatively calmer" with "weaker"
We have made the recommended change.

Line 407: BC diurnal behavior at NCOP(reported by Marinoni et al., ACP, 2010 and not by Bonasoni et al., 2010) is not bimodal but characterized by a single peak in late afternoon/evening.
We thank the reviewer for this point and have corrected the text to reflect this different behavior. The corrected text now reads: "The bimodal diurnal distribution of BC concentration in Jomsom is similar to that observed in Kathmandu (Putero et al. 2015) and unlike a singular late afternoon/evening peak seen at high elevation sites (Bonasoni et al., 2010) during non-monsoonal seasons. This illustrates that deep Himalayan valleys are susceptible to diurnal pollution similar to that of urban areas like Kathmandu. The morning peak is most likely due to local pollutants (from household and morning aircraft traffic) in Jomsom and settlements downwind of Jomsom, while the afternoon peak is associated with

long range transport. At the same time, O_3 exhibits a distinct minimum in the early morning with concentrations increasing towards an early afternoon peak – occurring well before BC's afternoon peak. The O_3 minimum in the morning further supports that the morning BC peak originates from local sources, as O_3 is only formed downwind of pollution sources. Further, the Jomsom station measuring BC and O_3 (JSM_STA) is located more than 100 m above the valley floor where the village of Jomsom sits. As such, we do not expect that local evening emissions would reach the stations at the cessation of up-valley flows and that evening drainage flows, following the valley floor would remove these local evening emissions down-valley.".

Line 418: "the distribution of BC concentrations…"..maybe " the differences of BC concentrations…"?
The revised sentence now reads: "The differences in BC concentration between up-valley and down-valley flows are statistically significant for all seasons (Figure 7a)."

Figure 7: I would say that DV fluxes must be negative…

Line 437: from Supplementary figure 1, wind speed at JSM_2 is more than 5 m/s higher than at JSM_1 (which is about 30%). Hardly you can define them "similar"… Please uniform station codes with Figure 2.
The reviewer makes a good point which we did not explain adequately in our previous version. We have acknowledged this difference and provided further justification for our approach. The text now reads: "Egger et al. (2000) used theodolite measurements to demonstrate uniform wind speeds within the bottom 1000m above the KGV floor at Jomsom and other locations. While we observed differences in wind speed of ~5 m s^{-1} between the two Jomsom stations during the limited times when data were available from both, we were unable to determine whether this pattern persisted throughout the year. For this reason, our only option is to follow the findings of Egger et al. (2000) and assign the wind speed at JSM_2 to the entire flux plane.".

Line 440: please provide formula for this calculation. Which is the usefulness of calculating this values of mass exported per day? Flux is defined as "kg/m2·s": "kg /day" is not a flux! Please revise.
We have now provided a description of our flux calculations (including the formula) in the methods section. We have now also corrected our values and units as pointed out by the reviewer.

Line 570: so, which is the outcome of this comparison? Table 1: Are std.dev or 95th confidence levels reported?
We have removed this text. We have clarified the table caption to indicate that the reported values are mean and standard deviation.

Figure 7: what the whiskers and bars represent?
The figure caption has been edited to include a more detailed description of the what the

whiskers and bars represent. The revised figure caption now reads: "Figure 7. (a) BC concentration distribution with down-valley (Dv) and up-valley (Uv) flows in Jomsom, (b) calculated Dv and Uv flux for each season, (c) Net daily flux per season. The dotted line is panel c marks 0 mg m^{-2} day^{-1}. The red line represents 50^{th} percentile, the edge of the box 25^{th} and 75^{th} percentile while the whiskers show maximum and minimum values.".

Supplementary Table 2: no measurement units are reported. Please adopt a nomenclature compliant with Figure 7
The table description now includes abbreviations consistent with Figure 7.

Supplementary Table 3 . this should be moved to the main manuscript! For each episode provide information about O3: when is it above the 90th percentile? When "cloud cover" is reported, did you mean that source identification was not possible? Please explain the manuscript text…
We have moved Supplementary Table 3 to the main text (Table 3). We removed MODIS imagery data as it was not comprehensive.

Reviewer #2

The present manuscript explores air quality data from a remote valley location in the Himalayas and tries to suggest that deep Himalayan valleys may act as important export routes for pollution from the Indo-Gangetic Plain (IGP) to the Tibetan Plateau (TP). The authors have addressed several comments given for the previous version of the manuscript and added some additional analysis. However, they fail to dissolve many of the major remarks made previously and the presented results still do not indisputably support the conclusions drawn by the authors. In addition, the technical quality of the manuscript has not improved and does not meet ACP standards (language, presentation of results). Therefore, I would suggest to reject the manuscript in its current for and encourage the authors to take the extensive comments made by reviewer 1 more seriously and carefully rework the manuscript for a novel submission.

We thank the reviewer for his/her continued and valuable feedback with our manuscript. We have made every effort to thoroughly address the remaining issues raised by Reviewer #1 and have made a global and thorough revision of the text's structure and grammar. As the primary goal of this manuscript is observational, we have also exercised greater caution in presenting the more speculative and preliminary aspects (i.e., flux estimates) of our work and have eliminated an examination of pollutant source regions. Taken together, these changes as well as the one's informed by the remaining comments of Reviewer #2 have helped to greatly strengthen our manuscript. Our responses to the reviewer's specific comments can be found below.

Specifically, I have three major concerns with the present study that would need to be addressed more adequately before the manuscript could be considered for publication.

Local influences

The local environment of the site and how local emissions may influence the present results and conclusions needs way more attention. A quick look on google Earth revealed that the town of Jomsom is not that small at all and that there is even a small airfield. A map (or googleEarth image) to clarify the site location relative to local pollution sources would be helpful to exclude any bias of the measurements due to local contamination. It would be possible to use the local wind observations to eliminate phases when local emissions directly influence the measurements. As the authors themselves state, the observed morning peak in BC is most likely due to local emissions from biofuel burning. The same might be true for the evening peak, but is never considered. Next to the local emissions also emissions further down the valley should be carefully looked at before concluding that all the observed BC is advected from the IGP rather than from the valley itself.

We have added text to better justify that the evening peak is dominated by non-local sources. The added text now reads: "Further, the Jomsom station measuring BC and O_3 (JSM_STA) is located more than 100 m above the valley floor where the village of Jomsom sits. As such, we do not expect that local evening emissions would reach the stations at the cessation of up-valley flows and that evening drainage flows, following the valley floor would remove these local evening emissions down-valley.".

Flux calculation

In the revised manuscript the authors present an estimate of the BC flux through the valley. Although it is never stated how this flux was calculated, I assume the authors multiplied the local wind speed and concentration measurements to derive a flux. This is really oversimplifying the transport situation in a complex alpine valley! At least vertical profiles of wind speed and concentrations would be needed to derive a robust flux estimate, two-dimensional transects would be even better.

Especially the nighttime flux at the near-surface site cannot be seen as representative for the whole valley atmosphere, since the surface layer often decouples from the flow above and considerable drainage flows may exist above. The idea to present a flux estimation to corroborate their conclusion of net pollution export through the valley is honourable but the present database simply does not allow for a robust estimate of a flux.

We agree with the reviewer that our flux estimate is preliminary and coarse. While the flux estimate is not central to our study, the estimate that we present is meant as a rough, initial, order-of-magnitude assessment. We have now included a description and formula for our flux calculations (as well as the assumptions that informed our estimate) in the methods section. Having clearly listed these limitations and assumptions in the text, if the reviewer or editor still has objections to this calculation, we can remove this aspect of the paper if necessary. The added text now reads: "Up-valley and down-valley BC fluxes were calculated separately

and determined using wind direction measurements. Instantaneous flux at time t was calculated as:

$$j_t = BC_t ws_t$$

where BC_t is the BC concentration (mg BC m^{-3}) at time t and ws_t is the wind speed (m hr^{-1}) at time t. From this, net daily mass transport (M_d) for day d was estimated as:

$$M_d = A\left(\sum\left(\frac{1}{6}j_{t,up}\right) - \sum\left(\frac{1}{6}j_{t,down}\right)\right)$$

where A is the cross-sectional area of the valley at Jomsom (1.41×10^6 m^2), $j_{t,up}$ and $j_{t,down}$ are the instantaneous up-valley and down-valley fluxes, respectively, occurring during day d, and the factor of 1/6 is the length of each time step in hours (i.e., 10 minutes divided by 60 minutes). The cross-sectional area was estimated as a trapezoid with a height of 800 m (the difference in elevation between the two Jomsom stations) and cross-valley distances of 800 m (at JSM_1) and 2720 m (at JSM_2). The average of these two cross-valley distances (1760 m) multipled by the height (800 m) yields the cross-sectional area of 1.41×10^6 m^2.

If we assume that (1) the polluted boundary layer within the valley at Jomsom is 800 m deep (i.e., the approximate elevational difference between the two AWS sites at Jomsom), (2) BC within the polluted boundary layer is well mixed, and (3) wind velocities do not vary significantly with altitude through the polluted layer, the mass flux BC through a vertical plane across the valley can be estimated. Supplementary Figure 1 shows that JSM_2 is well within the polluted haze layer during daytime/upvalley flows and that some BC is almost certainly transported above 800 m elevation. In this way we ensure that our estimates are conservative. The long lifetime of particulate BC against deposition (several days to a week or more) coupled with turbulent flow within the valley supports the assumption that BC is well mixed. In addition, Egger et al. (2000) used theodolite measurements to demonstrate uniform wind speeds within the bottom 1000m above the KGV floor at Jomsom and other locations. While we observed differences in wind speed of ~5 m s^{-1} between the two Jomsom stations during the limited times when data were available from both, we were unable to determine whether this pattern persisted throughout the year. These data limitations also prevented us from a more in-depth assessment of potential nighttime decoupling. For these reasons, our only option was to follow the findings of Egger et al. (2000) and assign the wind speed at JSM_2 to the entire flux plane.".

Trajectories

The presented analysis of trajectories and fire hot spots seems a bit arbitrary. The description of the back-trajectories is completely insufficient, both in terms of how they were calculated as well as how they are interpreted. The authors need to explain where and when the trajectories were initialized and why. Apparently the underlying meteorological data used for their calculation was insufficient to include the up-valley flow. So what was the meteorology used? The authors need to argue why it would be sufficient to include the transport from the

source regions to the valley mouth in any detail if model resolution is insufficient to cover the valley flow. The connection with the sources is too qualitative and vague to be used as evidence. The shown MODIS fire pixels can only be seen as an indication that there were some fires in the region, but they don't tell us anything about the absolute emission strength nor the relative emission strength during the whole observation period. More quantitative products of fire emissions are freely available and should be looked at (e.g., GFED, CAMS GFAS).

We have eliminated any assessment of pollution source. To do a thorough assessment would be beyond the scope of this paper. As such, we have included recommendations that future studies should examine this aspect, but now do not make any attempt to characterize pollution sources here.

Transport of regional pollutants through a remote trans-Himalayan valley in Nepal

Shradda Dhungel[1], Bhogendra Kathayat[2], Khadak Mahata[3], Arnico Panday[1,4]

[1] Department of Environmental Sciences, University of Virginia, Charlottesville, VA 22904, USA
[2] Nepal Wireless, Shanti Marg, Pokhara, 33700, Nepal
[3] Institute for Advanced Sustainability Studies, Potsdam, 14467, Germany
[4] International Center for Integrated Mountain Development, Khulmaltar, Kathmandu, 44700, Nepal

Correspondence to: Shradda Dhungel (shradda@virginia.edu)

Abstract. Anthropogenic emissions from the combustion of fossil fuels and biomass in Asia have increased in recent years. High concentrations of reactive trace gases and light-absorbing and ~~light~~-scattering particles from these sources over the Indo-Gangetic Plain (IGP) of southern Asia form persistent haze layers, also known as atmospheric brown clouds, from December through early June. Models and satellite imagery suggest that strong wind systems within deep Himalayan valleys are major pathways by which pollutants from the IGP are transported to the higher Himalaya yet observational evidence of transport through Himalayan valleys has been lacking to date. To evaluate this pathway, we measured black carbon (BC), ozone (O_3), and associated meteorological conditions within the Kali-Gandaki Valley (KGV), Nepal, from January 2013 to July 2015. BC and O_3 varied over both diurnal and seasonal cycles. Relative to nighttime, mean BC and O_3 concentrations within the valley were higher during daytime when the up-valley flow (average velocity of 17 m s^{-1}) dominated. BC and O_3 concentrations also varied seasonally with minima during the monsoon season (July to September). Concentrations of both species subsequently increased post monsoon and peaked during March to May. Average concentrations for O_3 during April, August, and November were 41.7 ppbv, 24.5 ppbv, and 29.4 ppbv, respectively, while the corresponding BC concentrations were 1.17 µg m^{-3}, 0.24 µg m^{-3}, and 1.01 µg m^{-3}, respectively. Up-valley fluxes of BC ~~fluxes~~ were significantly greater than down-valley fluxes during all~~each~~ seasons. In addition, frequent episodes of BC concentrations two to three times~~fold~~ higher than average persisted from several days to a week during non-monsoon months. Our observations of increases in BC concentration and fluxes in the valley, particularly during ~~preceding the~~pre- monsoon, ~~and in conjunction with widespread agricultural burning and wildfires over the IGP,~~ support the hypothesis that trans-Himalayan valleys are important conduits for transport of pollutants from the IGP to TP.

Keywords: black carbon, ozone, trans-Himalayan valleys, pollutant pathways, long-range transport, regional transport episodes, short-lived climate forcers.

1. Introduction

Persistent atmospheric haze, often referred to as Atmospheric Brown Cloud~~s~~ (ABC) (Ramanathan and Crutzen, 2003), affects broad geographic regions including the Indo-Gangetic plain (IGP) in southern Asia (Ramanathan and Carmichael, 2008), eastern China (Ma et al., 2010), southeast Asia (Engling and Gelencser, 2010), sub-Saharan Africa (Piketh et al., 1999), Mexico (Vasilyev et al., 1995), and Brazil (Kaufman et al., 1998). In southern Asia, the haze covers extensive areas particularly during the period of mid-November to mid-June preceding the summer monsoon season. Major combustion sources (primarily anthropogenic) including ~~wildfires and~~ the burning of agricultural waste, garbage, biofuel, and fossil fuels as well as wildfires emit volatile and particulate-phase compounds to the atmosphere that contain oxidized and reduced forms of sulfur, nitrogen, and organic carbon (OC) together with elemental (black) carbon (BC) and other species. These emissions are intermixed and chemically interact with mechanically produced aerosols (e.g., sea salt and mineral dust). Important secondary pollutants such as ozone (O_3) form from photochemical reactions involving nitrogen oxides and volatile organic species are also produced. Together, this mixture of atmospheric species constitutes ABC or the brown haze in South Asia (Ramanathan et al., 2005; Gustafsson et al., 2009). These optically thick layers include high concentrations of light absorbing and light scattering particles (Menon et al., 2002) that modulate radiative transfer. Light absorbing aerosols (primarily BC and crustal dust) contribute to warming of the atmosphere while light scattering aerosols (primarily S-, N-, and OC dominated particles) drive cooling at the surface. The combined effects of light absorbing and light scattering aerosols from anthropogenic sources reduce UV and visible wavelength radiation at the surface (i.e., surface forcing), increase the warming of the troposphere (i.e., atmospheric forcing) and change the net top of the atmosphere solar flux (i.e., top-of-the-atmosphere forcing) (Andreae and Crutzen, 1997; Kaufman et al., 2002, Ramanathan et al., 2005). Light-a~~A~~bsorbing anthropogenic pollutants like BC significantly influence global warming, in terms of direct radiative forcing (Jacobson, 2001; Bond et al., 2013); regional influences from such pollutants close to sources are greater than those on the global scale (Ramanathan et al., 2007b).

The elevated concentration of aerosols in the anti-cyclone also weakens the circulation pattern and reduces total monsoon precipitation over southern India (Ramanathan et al, 2005; Fadnavis et al., 2013) while intensifying the monsoon over the foothills of the Himalaya (Lau et al., 2006). In addition to

warming the atmosphere, the rising concentrations of BC and O_3 over southern Asia (e.g., Ramanathan and Carmichael, 2008) have detrimental impacts on human health. The effects of BC on cardiopulmonary and respiratory problems are greater than those of PM 2.5 or 10 particles (Janssen et al., 2011). O_3 also compromises pulmonary function (Krupnick et. al, 1990) and is a leading pollutant causing biodiversity loss (Royal Society, 2008) and declining crop yields by directly damaging leaves (Auffhammer et al., 2006).

Most haze over the IGP often reaches heights of more than 3 km above sea level via convection and advection, and the Himalaya range forms a 2500 km long, 8 km high complex topographic barrier along the northern edge of the IGP (Singh et al., 2004; Dey and Di Girolamo, 2010; Gautam et al., 2011). Numerous studies have investigated the ~~possibility of the~~ transport of pollutants from the IGP to the Himalayan foothills, the immediate source region for potential transport to the Tibetan Plateau (TP) (Pant et al., 2006; Dumka et al., 2008; Komppula et al., 2009; Hyvärinen et al., 2009; Ram et al., 2010; Brun et al., 2011; Gautam et al., 2011; Srivastava et al., 2012). ~~extending more than 8 km high.~~ Further~~However~~, a suite of studies involving satellite imagery (Ramanathan et al., 2007a, Brun et al., 2011), back trajectories (Lu et al., 2011), model calculations (Kopacz et al., 2011), ice core analyses (Lee et al., 2008, Kang et al., 2010), and measurements in the higher Himalaya (Bonasoni et al., 2010) strongly suggest that pollutants are efficiently transported from the IGP to the higher Himalaya and onto the Tibetan Plateau, especially during spring prior to the monsoon. -Absorbing aerosols warm the atmosphere at high altitudes and, when deposited onto snow and ice surfaces, decrease albedo thereby substantially increasing the rate of glacial and snow melting (Kang et al., 2010). Model simulations (Qian et al., 2011) show that the absorbing aerosols change the surface radiative flux in the higher Himalaya and the TP by 5 to 25 W m^{-2} during the pre-monsoon months of April and May. The TP plays a vital role in regulating the regional climate due to its effect on the Asian summer monsoon (ASM) and the hydrologic cycle. The interrelated perturbations of the ABC on radiative transfer, air quality, the hydrologic cycle, and crop yields have important long-term implications for human health, food security, and economic activity over southern Asia.

~~Lüthi et al. (2015) found that synoptic circulation patterns, in combination with local weather phenomena, are associated with the transport of polluted air masses from the IGP to the TP. Several major Himalayan valleys including the Arun Valley in eastern Nepal and the Kali Gandaki Valley (KGV) in western Nepal provide topographical connections for air masses from the south to the TP (Fig.1). In addition to synoptic transport over the Himalaya, MODIS (MODerate resolution Imaging Spectroradiometer) and CALIPSO (Cloud-Aerosol Lidar and Infrared Pathfinder Satellite Observation) imagery reveal northward slanted transport of polluted air mass towards higher elevations in the Arun~~

~~Valley (Brun et al, 2011).~~ However, to date, there has been little observational research to directly demonstrate ~~understand~~ the role of mountain valleys in the transport of~~on how~~ air pollutants from the IGP and the Himalayan foothills to higher elevations within and north of the Himalayan range. ~~flow through the topographic barrier.~~

In other studied mountain ranges, it is w~~W~~ell k~~-k~~nown that flow patterns carry polluted air masses up valleys to higher elevations by providing a path of least resistance between tall mountains. In the European Alps, prevailing wind systems in the mountain river valleys funnel polluted air from peripheral source regions to high elevations in a phenomenon known as "Alpine Pumping" (Weissmann et al., 2005). Under fair weather conditions during daytime, the upslope winds are capable of transporting significant pollutants and moisture into the free troposphere (Henne et al., 2004). Relative to air over plains, the air within the valley heats and cools more quickly (Steinacker, 1984). The resultant differences in temperature create gradients in pressure and density, which in turn drive transport of air from the plains to higher-elevations during the daytime (Reiter and Tang 1984, Whiteman and Bian, 1998; Egger et al., 2000). Such direct evidence of a Himalayan mountain valley wind system and its role in pollution transport has yet to be observed. ~~Numerous studies have investigated the possibility of the transport of pollutants from the IGP to the Himalayan foothills (Pant et al., 2006; Dumka et al., 2008; Komppula et al., 2009; Hyvärinen et al., 2009; Ram et al., 2010; Brun et al., 2011; Gautam et al., 2011; Srivastava et al., 2012).~~ ~~Other studies show that pollutants have the potential to reach not only the foothills of the Himalaya but also higher elevations (Bonasoni et al., 2010; Decesari et al., 2010; Marinoni et al., 2010).~~Studies in the Himalayan region have looked into the transport of pollutants across the mountains (Lüthi et al., 2015) and the contribution of region sources like open fires to the occurrence of ABC (Ramanathan et al., 2005; Ramanathan and Crutzen, 2003). ~~In addition, studies have shown the obstruction of flow caused by the high Himalaya which intensifies the effect of pollution over the IGP that are visible in satellite imagery especially during pre-monsoon seasons (Singh et al., 2004; Dey and Di Girolamo, 2010; Gautam et al., 2011).~~ ~~Other studies show that pollutants have the potential to reach not only the foothills of the Himalaya but also higher elevations (Bonasoni et al., 2010; Decesari et al., 2010; Marinoni et al., 2010).~~ ~~Though there is evidence of existence of similar source pollutants, both regional and local, in the foothills and the higher altitude sites (Raatikainen et al., 2017; Raatikainen et al., 2014; Srivastava et al., 2012,), observational evidence of Himalayan valleys as mechanisms and possible pathways facilitating such transport via Himalayan valleys is lacking.~~ Here we present 2.5 years of measurements of BC, O_3, and associated meteorological data from one of the deepest trans-Himalayan valleys, the Kali-Gandaki Valley. We examine seasonal and diurnal patterns of BC and O_3, investigate potential episodes of enhanced pollution transport up-valley, and make a preliminary estimate of BC mass transport. In doing so, we seek to provide the first

Formatted: Subscript

observational evidence of trans-Himalayan valleys acting as conduits for pollution transport from the IGP to the higher Himalaya ~~TP. Our data fills this gap by characterizing~~illustrates the importance of ~~Himalayan valleys as channels of pollutant transport the role of the wind system within a deep Himalayan valley in transporting pollutants from the IGP to the high mountains~~deep Himalayan valleys ~~with the help of local wind system.~~

2. Measurement Sites and Methods

2.1 Measurement Sites and Instrumentation

This paper presents data from an atmospheric measurement station in Jomsom (28.87° N, 83.73° E, 2900 m asl) within the core region of the KGV along with four other automated weather stations up and down the valley from Jomsom. With the exception of aerosol optical depth measured as part of AERONET (AErosol RObotic NETwork) (Xu et al., 2015), no pollution data from Jomsom have been previously reported previously. Here we report diurnal and seasonal trends in two ~~climatically~~ important ~~pollutants~~ SLCPs – BC and O_3 – to ~~. Results are interpreted to~~ evaluate the role of trans-Himalayan valleys as pathways for the transport of polluted air from the IGP to the higher Himalaya.

The KGV is located in the Dhaulagiri zone of western Nepal (Fig. 1(a)). ~~Figure 1(a), shows the TP in the upper right, with the Himalayan arc, the Himalayan foothills of India, and Nepal, and the haze covered Himalayan foothills. The intrusion of haze into Himalayan valleys is clearly visible.~~ The KGV floor changes elevation from approximately~~.~~ 1100 m to 4000 m above sea level (asl) over a horizontal distance of 90 km (Fig. 1(b)). Passing between the two eight thousand meter peaks of Dhaulagiri and Annapurna, it forms one of the deepest valleys in the world. The valley is a narrow gorge at the lower end and opens up into a wider, arid basin ~~half way up~~ (Fig. 1(b)) with a~~. The~~ maximum width of ~~the basin is~~ approximately one kilometer. The orientation of KGV varies from the entrance to the exit. The ~~valley is oriented~~ general orientation ~~i~~of the valley is ~~southeasterly~~ from SW~~E (~135°)~~ (the mouth of the valley) to ~~northwesterly~~ NE ~~(~315°)~~ ~~at the bottom~~ (the head of the valley) (Fig. 1).~~. The valley's orientation changes to southwesterly (~225°) to northeasterly (~45°) at the core of then turns north (~20°) past the core of the valley (Fig. 1).~~ Approximately 13,000 inhabitants in several small settlements sparsely populate the valley. Emission sources within the valley include biofuel combustion for cooking and fossil-fuel combustion by off-road vehicles. There is an airport in Jomsom which operates only in the morning as narrow valley width and high up-valley wind speeds make it dangerous for small aircraft to land at other times. A total of 5245 vehicles have been registered in Dhaulagiri Zone since 2008, but most are based in the southern towns of Kusma, Baglung, and Beni, below 1 km

altitude, at the lowest left corner of the map in Figure 1(b) (DOTM, 2016).

The atmospheric observatory at Jomsom (JSM_STA) is equipped with instruments to measure BC, O_3, and meteorology (Figure 2). The observatory is located on the southeast corner of a plateau jutting out from an east-facing slope about 100 m above the valley floor and with no major obstructions either up or down the valley. Equivalent black carbon (hereafter referred to as BC) was measured with a Thermo Multiangle Absorption photometer (MAAP), model 5012 that uses a multi-angle photometer to analyze~~s~~ the modification of radiation fields – as caused by deposited particles that entered through a straight, vertical inlet line – in ~~in~~ the forward and back hemisphere of a glass-fiber filter (GF-10). ~~caused by deposited particles using a multi-angle photometer.~~ MAAP was operated at a flow rate of 20 L min^{-1}, ~~and~~ measuring~~s~~ BC at 1-minute frequency. We note that Hyvärinen (2013) illustrates the artifact in MAAP measurements in environments with high aerosol loading with an underestimation of concentration above 9 µg m^{-3}. Since the median monthly concentrations for the duration of the measurement were less than 1µg m^{-3} and 90th percentile below 2 µg m^{-3} (and therefore below this threshold), ~~, which are below the threshold of 9 µg m^{-3},~~ MAAP corrections were not applied. O_3 was measured with a 2B Tech model 205 via the attenuation of ultraviolet light at 254 nm passing through a 15 cm long absorption cell fitted with quartz windows. The instrument was operated~~s~~ at a flow rate of 1.8 L min^{-1}. For instrument calibration, ~~T~~the BC instrument performed an automatic span and zero checks every 24 hours while zero checks on the O_3 instrument were~~as~~ performed every 7 days. Wind speed and direction were measured by an automated weather station installed on a ridge 900 m (JSM_2) above the sampling site for BC and O_3.

2.2 Data summary

The observatory operated from January 2013 through July 2015, but periodic power disruptions caused occasional data gaps (~~Supplementary~~ Table 1). Unless otherwise noted, data reported herein correspond to periods when BC, O_3, and meteorological data were available simultaneously. Data are binned by season as follows: monsoon (July-September), post-monsoon (October-February) and pre-monsoon (March-June). Times correspond to Nepal's local time (LT) (UTC + 5.75 h). From March to May 2015, four additional automated weather stations were operated along a transect roughly 10 meters above and in the center of the valley floor where wind speeds are typically the highest: near the entrance of the valley at Lete (LET), within the core at Marpha (MPH) and Jomsom (JSM_2), and near the valley exit at Eklobhatti (EKL) (Fig. 1b). Power outages, instrument malfunctions, and a major earthquake in Nepal on April 25th, 2015 (and its aftershocks) limited the duration~~s~~ of records at all sites. However, between 1st and 14th May, all stations operated simultaneously and the resulting data provide information with which to evaluate diurnal variability of wind fields along the valley.

Formatted: Subscript

Formatted: Font: Bold

Formatted: Font: (Intl) Calibri

BC, O_3, and meteorological data were averaged over 10 minute intervals. Up-valley (southwesterly) flows are defined as between 35° and 55° while down-valley (northeasterly) flows include data between 215° and 235°. Data for all days for which complete data were available over entire 24-hour periods were binned by season. The statistical significance of differences between up-valley and down-valley flow conditions during different seasons were evaluated using the non-parametric Kruskal Wallis and Mann-Whitney tests.

To normalize for the influence of day-to-day variability in absolute concentrations, relative diurnal variability in O_3 and BC concentrations measured during a given month were normalized to a common scale ranging from 0 to 1 (see e.g., Sander et al., 2003; Fischer et al., 2006). Normalized BC values for month *m* were calculated as:

$$BC_{n,t} = \frac{BC_t - \min BC_m}{\max BC_m - \min BC_m}$$

where BC_t is the BC concentration at time *t* in the month *m*, and $\max BC_m$ and $\min BC_m$ are the maximum and minimum BC concentrations observed during month *m*. The normalized data were then binned into twenty-four, hourly increments. These calculations were repeated for O_3.

2.3 Preliminary flux estimates

Up-valley and down-valley BC fluxes were calculated separately and determined using wind direction measurements. Instantaneous flux at time *t* was calculated as:

$$j_t = BC_t ws_t$$

where BC_t is the BC concentration (mg BC m^{-3}) at time *t* and ws_t is the wind speed (m hr^{-1}) at time *t*. From this, net daily mass transport (M_d) for day *d* was estimated as:

$$M_d = A\left(\sum\left(\frac{1}{6}j_{t,up}\right) - \sum\left(\frac{1}{6}j_{t,down}\right)\right)$$

where *A* is the cross-sectional area of the valley at Jomsom (1.41×10^6 m^2), $j_{t,up}$ and $j_{t,down}$ are the instantaneous up-valley and down-valley fluxes, respectively, occurring during day *d*, and the factor of 1/6 is the length of each time step in hours (i.e., 10 minutes divided by 60 minutes). The cross-sectional area was estimated as a trapezoid with a height of 800 m (the difference in elevation between the two

Formatted ...
Formatted ...
Formatted ...
Formatted ...
Formatted ...
Formatted ...
Formatted ...
Formatted ...
Formatted ...
Formatted ...
Formatted ...
Formatted ...
Formatted ...
Formatted ...
Formatted ...
Formatted ...
Formatted ...
Formatted ...
Formatted ...
Formatted ...
Formatted ...
Formatted ...
Formatted ...
Formatted ...
Formatted ...
Formatted ...
Formatted ...
Formatted ...
Formatted ...
Formatted ...
Formatted ...
Formatted ...
Formatted ...
Formatted ...
Formatted ...
Formatted ...
Formatted ...
Formatted ...
Formatted ...

Jomsom stations) and cross-valley distances of 800 m (at JSM_1) and 2720 m (at JSM_2). The average of these two cross-valley distances (1760 m) ~~multiplied~~multiplied by the height (800 m) yields the cross-sectional area of 1.41×10^6 m^2.

If we assume that (1) the polluted boundary layer within the valley at Jomsom is 800 m deep (i.e., the approximate elevational difference between the two AWS sites at Jomsom), (2) BC within the polluted boundary layer is well mixed, and (3) wind velocities do not vary significantly with altitude through the polluted layer, the mass flux BC through a vertical plane across the valley can be estimated. Supplementary Figure ~~2~~1 shows that JSM_2 is well within the polluted haze layer during daytime/upvalley flows and that some BC is almost certainly transported above 800 m elevation. In this way we ensure that our estimates are conservative. The long lifetime of particulate BC against deposition (several days to a week or more) coupled with turbulent flow within the valley supports the assumption that BC is well mixed. Supplementary figure 2 shows that the potential temperature (theta) gradient is less than zero between JSM_1 and JSM_2 which illustrates that the air within the valley is unstable. In addition, Egger et al. (2000) used theodolite measurements to demonstrate uniform wind speeds within the bottom 1000m above the KGV floor at Jomsom and other locations. While we observed differences in wind speed of ~5 m s^{-1} between the two Jomsom stations during the limited times when data were available from both, we were unable to determine whether this pattern persisted throughout the year. These data limitations also prevented us from a more in-depth assessment of potential nighttime decoupling. For these reasons, our only option was to follow the findings of Egger et al. (2000) and assign the wind speed at JSM_2 to the entire flux plane.

3. Results and Discussion

3.1 Evolution of local wind system in the KGV

An understanding of the local wind regime is essential for analyzing pollution transport through mountain valleys. Measurements from JSM_2 show the diurnal evolution of wind at Jomsom in each season. All data collected were used to analyze the diurnal pattern of wind at Jomsom (Fig. 3a, 3b, 3c). Wind roses illustrate the temporal evolution of up- and down-valley flows at JSM_2 for each season. At JSM_2, up-valley flows are southwesterly and dominant during daytime, with peak velocities above 15 m s^{-1} between 0900 LT to 1800 LT. Wind velocities decreased substantially after 1800 LT, with variable wind direction until midnight, followed by northeasterly winds (during pre- and post-monsoon seasons (Fig. 3a and 3c)). The wind patterns during monsoon appear strongly influenced by the monsoon anticyclone; this observation is in agreement with wind direction measurements from other

Formatted: Superscript

Formatted: Superscript

Himalayan valleys (Bonasoni et al., 2010; Ueno et al., 2008) (Fig. 5b). Although wind velocities at JSM_2 varied over the year, non-monsoon months exhibited similar diurnal patterns that evolved seasonally as a function of sunrise and sunset (Fig. 3a, 3b, 3c), characteristics which were exhibited in the monsoon season. As discussed below, this alternating pattern in wind direction from strong daytime flows to weak nighttime flows during dry months results in a net transport of pollutants up the valley.

Our measurements at the four AWS stations on the valley floor illustrate the evolution of surface wind velocities along the length of the KGV (Supplementary Figure 3). In general, wind speeds along the valley floor were strongest within the core of the valley at MPH, JSM_1 and JSM_2 and were lower in the entrance (LET) and exit (EKL) regions (Supplementary Figure 3). The duration of strong wind speeds within the valley during daytime is consistent with the hypothesis that wind patterns are modulated by the pressure gradient created as a result of differential heating of the arid valley floor relative to the mouth of the valley (Egger et al, 2000). In addition, comparison of measurements at JSM_1 and JSM_2 (Fig. 3a, 3b, 3c and Supplementary Figure 3) provided information regarding vertical variability in wind speed. Velocities at the higher elevation site of JSM_2 were about 5 m s^{-1} and 3 m s^{-1} greater than those near the valley floor during daytime and nighttime, respectively. The two sites exhibited similar diurnal cycles with the exception of a relatively stronger northeasterly wind at JSM_2 from 0300 to 0900 LST.

~~3.1 Seasonal variability in BC and O_3~~

~~All data generated during the measurement period were binned by month to evaluate the seasonal patterns of BC and O_3 (Fig. 3). IOn addition, individual months with the most complete data coverage during the pre-monsoon (April 2013), monsoon (August 2014), and post-monsoon (November 2014) seasons were selected to evaluate aspects of temporal variability in greatermore detail (Fig. 4).in the presence and absence of Based on median values, the highest concentrations of both species occurredwere during the months preceding the monsoon and the lowest were during months of the monsoon. We infer that Tthe significantly lower concentrations during the monsoon reflect the combined influences of synoptic easterly airflow that transports a cleaner marine air mass over the region, reduced agricultural residue burning (Sarangi et al., 2014), and more efficient aerosol removal via wet deposition (Dumka et al., 2010). during the monsoon seasonO_3 production is also suppressed under increased cloudinessy conditions during the monsoon may also reduce O_3 production (Lawrence and Lelieveld, 2010). Similar seasonal variability in BC concentration is evident across the IGP from urban to remote locations. For example, high concentrations of BC (~1.48 to 1.99 µg m^{-3}) have been~~

reported in near-surface air across the IGP as well as in layers of the atmosphere at ~900 m asl and ~1200 m asl during the post-monsoon over Northern India (Tripathi et al, 2005; 2007). Sreekanth et al (2007) reported BC concentrations in Vishkhapatnam, in eastern India, to be 8.01 μg m^{-3} in pre-monsoon and 1.67 μg m^{-3} during monsoon while Ramchandran et al (2007) observed BC concentrations in Ahmedabad, western India, of 0.8 μg m^{-3} during the monsoon in July to 5 μg m^{-3} during the post monsoon in January. Similar seasonable variability has also been reported in the high Himalaya however the peak occurs later between in the post-monsoon season in March-April.

The post-monsoon timing of peak BC concentrations observed in previous studies performed in the IGP and Himalayan foothills (see e.g., Tripathi et al, 2005; 2007; Ramchandran et al., 2007; Putero et al, 2015) differs from our observations in the KGV, where we see heightened BC during the pre-monsoon season (Fig. 4). These findings are generally For example, the Nepal Climate Observatory-Pyramid (NCO-P) station at the 5079 m asl in the Himalaya has also shown high seasonal differences for BC and O_3 between pre-monsoon (0.444 (±0.443) μ g BC m^{-3}; 61 (±9) ppbv O_3) and during pre-monsoon and monsoon (0.064 (±0.101) μ g m^{-3}; 39 (±10) ppbv O_3) during monsoon season and ozone concentrations 61 (±9) ppbv during pre-monsoon season and 39 (±10) ppbv during monsoon (Cristofanelli et al., 2010, Marinoni et al., 2013) (Table 1). Our results therefore indicateindicate a lagged peak that seasonable variability in BC and O_3 within the KGV and presumably other deep Himalayan valleys, as compared to sites within the IGP. is coupled with these larger regional-scale patterns.

3.2 Diurnal variability in BC and O_3

To normalize for the influence of day-to-day variability in absolute concentrations, relative diurnal variability in O_3 and BC concentrations measured during a given month were normalized to a common scale ranging from 0 to 1 by subtracting the minimum for the month from each individual value and then dividing by the range for the month (e.g., Sander et al., 2003; Fischer et al., 2006). The data were then binned into twenty-four, 1-hour increments and plotted (Fig. 54).

Based on median values during all three periods, O_3 peaked during daytime and dropped to minimal levels before sunrise during all three study seasons (pre-monsoon, monsoon, and post-monsoon. However, in April 2013the (pre-monsoon period) O_3 peaked in the late afternoon whereas in November 2014the (post-monsoon), it peaked in the early afternoon. In addition, the normalized diurnal excursions were greater during the pre- and post-monsoon periods relative to the monsoon period – represented by August 2014.July 2015. In contrast, based on median values during all three periods, BC concentrations increased rapidly in the early morning, decreased during late morning, and then rose again through the afternoon and early evening hours (Fig. 54). Relative diurnal variability was

somewhat greater during post-monsoon~~the post-monsoonNovemeber 2015~~ relative to the pre-monsoon and monsoon periods.~~ the pre-monsoon periodsApril 2013 and lower during the monsoon periodJuly 2015.~~ Across all seasons, ~~T~~the lower normalized distributions ~~more skewed distributions~~ for BC relative to O_3 reflect infrequent periods of high BC concentrations.~~ during all three seasons.~~

Several factors likely contributed to differences in timing of the~~ in the diurnal variability of~~ daily peaks in O_3 and BC concentrations. These include potentially different source regions for BC and O_3 precursors, the timing of ~~diurnal variability in emissions of BC versus O_3 precursors and/or production in source regions followed by regional transport, diurnal variability in~~ the photochemical ~~chemical~~ production and destruction of O_3,~~ˀ~~ and contributions of O_3 ~~o~~and~~ɾ~~ its precursors from non-combustion sources like stratospheric ozone and biogenic hydrocarbons from vegetation. ~~O_3 is produced photochemically and is lost via deposition to surfaces and chemical reactions. In contrast, BC is a primary emission product of combustion that may originate from both local and distant sources.~~ The early morning BC peak during all ~~three~~ seasons suggests ~~probable~~ contributions from the local combustion of biofuels for cooking and heating, which are most prevalent during early morning. The secondary peak in the afternoon and early evening occurs when the local anthropogenic emission sources are at a minimum in the KGV.

Formatted: Font: (Intl) Times New Roman, Subscript

3.3 Seasonal variability in BC and O_3

All data generated during the measurement period were binned by month to evaluate the seasonal patterns of BC and O_3 (Fig. 5). In addition, individual months with the most complete data coverage during the pre-monsoon (April 2013), monsoon (August 2014), and post-monsoon (November 2014) seasons were selected to evaluate aspects of temporal variability in greater detail (Fig. 5). We divided the seasons into dry (pre-monsoon, post-monsoon) and wet (monsoon) seasons to understand the transport of pollutants via Himalayan valleys in the presence and absence of wet deposition processes. Based on median values, the highest concentrations of both species occurred during the months preceding the monsoon and the lowest were during months of the monsoon. The significantly lower concentrations during the monsoon reflect the combined influences of synoptic easterly airflow that transports a cleaner marine air mass over the region, reduced agricultural residue burning (Sarangi et al., 2014), and more efficient aerosol removal via wet deposition (Dumka et al., 2010). In addition to possible active wet deposition of O_3 precursors during the monsoon season, increased cloudiness during monsoon may also reduce O_3 production (Lawrence and Lelieveld, 2010).

The post-monsoon timing of peak BC concentrations observed in previous studies performed in the IGP and Himalayan foothills (see e.g., Tripathi et al, 2005; 2007; Ramchandran et al., 2007; Putero et al,

2015) differs from our observations in the KGV, where we see heightened BC during the pre-monsoon season (Fig. 5). These findings are generally in agreement with other high altitude observations. For example, the Nepal Climate Observatory-Pyramid (NCO-P) station at the 5079 m asl in the Himalaya has also shown high seasonal differences for BC and O_3 between pre-monsoon (0.444 (±0.443) µg m^{-3} BC; 61 (±9) ppbv O_3) and monsoon (0.064 (±0.101) µg m^{-3} BC; 39 (±10) ppbv O_3) (Cristofanelli et al., 2010, Marinoni et al., 2013) (Table 2). Our results therefore indicate a lagged peak in BC and O_3 within the KGV and presumably other deep Himalayan valleys, as compared to sites within the IGP.

~~3.3 Evolution of local wind system in the KGV~~

~~Aning of is essential for analyzing pollution transport through mountain valleys~~Measurements from JSM_2 ~~show the diurnal evolution of wind in each season. All data collected were used to analyze the diurnal pattern of wind at Jomsom (Fig. 6). The W~~wind roses ~~illustrate the temporal evolution of up- and down-valley flows at JSM_2 for each season (Fig. 6). At JSM_2, up-valley flows are southwesterly and dominant during daytime, with peak velocities above 15 m s^{-1} between about 0900 LT to 1800 LT. Wind velocities decreased substantially after 1800 LT, with variable wind direction until midnight, followed by then northeasterly winds are common (during pre- and post-monsoon seasons (Fig. 6a and 6c)). The wind patterns during monsoon appear~~was strongly influenced by the monsoon anticyclone~~;~~ ~~this observation is in agreement with wind direction measurements from other Himalayan valleys (Bonasoni et al., 2010; Ueno et al., 2008) (Fig. 6b). Although wind velocities at JSM_2 varied somewhat over the year, non-monsoon months exhibited similar diurnal patterns that evolved seasonally as a function of sunrise and sunset (Fig. 6), characteristics which were exhibited unlike in the monsoon season. As discussed below, this alternating pattern in wind direction from strong daytime flows to weak nighttime flows during dry months results in a net transport of pollutants up the valley.~~

~~Theodolite observations at different locations along the KGV in 1998 show minor shifts – less than 45° – in wind direction and less than 2 m s^{-1} in wind speed in the lower 1000 m above the surface during daytime (Egger et.al 2000). Based on the average daytime wind speed, the valley can be partitioned into three regions: the entrance, core, and exit (average wind speeds range from 5 to 10 m s^{-1}, 8 to 18 m s^{-1}, and less than 5 m s^{-1}, respectively) (Egger et al 2000). The strongest winds within the core region are most prevalent in the lower 1000 to 1500 m of the boundary layer within the valley (Egger et al, 2000; Zängl et al., 2000, Egger et al., 2002). Our measurements at the four AWS stations on the valley floor illustrate the evolution of surface wind velocities along the length of the KGV (Supplementary Figure 1). In general, wind speeds along the valley floor were strongest within the core of the valley at MPH,~~

JSM_1 and JSM_2 and were lower in the entrance (LET) and exit (EKL) regions (Supplementary Figure 1). The duration of strong wind speeds within the valley during daytime is consistent with the hypothesis that wind patterns are modulated by the pressure gradient created as a result of differential heating of the arid valley floor relative to the mouth of the valley (Egger et al, 2000). In addition, comparison ofson between measurements at JSM_1 and between 1st and 14th May 2015 and the longer-term record JSM_2 for same period (Fig. 6 and Supplementary Figure 1) provided information regarding vertical variability in wind speed. Velocities at the higher elevation site of JSM_2 were about 5 m s^{-1} and 3 m s^{-1} greater than those near the valley floor during daytime and nighttime, respectively. the day and 3 m s^{-1}stronger at nighttime but with The two sites exhibited similar diurnal cycles with the exception of. While there is a relatively stronger northeasterly wind at JSM_2 from 0300 to 0900 LST, in comparison to JSM_1. Airflow along the valley is driven by gradients in temperature and pressure between the entrance and the exit regions of the valley (Egger, 2000). Wind speed along the valley floor peaked within the core of the valley at MPH, JSM_1 and JSM_2 and were lower in the entrance (LET) and exit (EKL) regions (Supplementary Figure 1). The duration of strong wind speeds within the valley during daytime is consistent with the hypothesis that wind patterns are modulated by the pressure gradient created as a result of differential heating of the arid valley floor relative to the mouth of the valley Egger et al. (2000).

3.43.1 Local winds as drivers of BC and O_3 transport in the KGV

Figure 4 6 shows the time series of BC and O_3 during individual months or in each seasons (April/pre-monsoon, August/monsoon, November/post-monsoon). For pre-monsoonApril, BC concentrations peaked at 0700 LST (Fig. 46) when wind velocities were low (Fig. 46). This peak occurred about an hour later during the post-monsoon periodin November, with all seasonsboth periods experiencing a decrease in BC over the rest of the morning as wind speeds increased and diluted local emissions (Fig. 45). Dilution of local emissions associated from increasing wind speed likely contributes to decreasing BC concentration during late morning. Thereafter, BC concentrations increased over the afternoon and early night, reaching secondary peaks near midnight LST during in the pre-monsoonApril and several hours earlier during other periods in November and August (Fig. 4 and 56). Distinct morning and afternoon peaks in BC concentration are seen in the post-monsoon season when the up-valley wind speeds are relatively calmer weaker than in pre-monsoon season (Fig. 5 4 and 6). The bBimodal diurnal distribution of diurnal BC concentration in Jomsom is similar to that observed in Kathmandu as reported by (Putero et al. (2015) butand unlike a singular late afternoon/evening peak in the late afternoon/evening inseen at high elevation sites (Bonasoni et al., 2010) where similarduring non-

monsoonal seasons. This illustrates that deep Himalayan valleys are susceptible to diurnal pollution similar to that of urban areasecities like Kathmandu. The morning peak in BC is most likely due to diurnal peaks were observed (Bonasoni et al., 2010; Hindman et al., 2002; Hegde et al., 2007). local pollutants (from household and morning aircraft traffic) in Jomsom and settlements downwind of Jomsom,. Wwhile the afternoon peak is likely primarily associated with long range in addition to local pollutants. At the same time, Simultaneously, O_3zone exhibits a distinct minimum in the early morning with concentrations increasing towards an early afternoon peak – occurring well before BC's afternoon peak. However, mixing ratios increase during the morning, peak in the early afternoon well before that of BC and decrease over night. The O_3 minimuma in the morning further supports that the morning BC peak originates from corroborates the role of local sources,pollutants responsible for morning peak as since O_3 is only formed downwind of pollution sources. Further, the Jomsom station measuring BC and O_3 (JSM_STA) is located more than 100 m above the valley floor where the village of Jomsom sits. As such, we do not expect that local evening emissions would reach the stations at the cessation of up-valley flows and that evening drainage flows, following the valley floor would remove these local evening emissions down-valley.

Formatted: Subscript

Formatted: Subscript

Formatted: Subscript

Percentage distributions of up-valley and down-valley BC concentrations, fluxes, and net daily fluxes per unit cross section are depicted in Figure 7 and summarized in Supplementary Table 21. Up-valley (southwesterly) flows are defined as between 35° and 55° while down-valley (northeasterly) flows include data between 215° and 235°. Date for all days for which complete data were available over entire 24-hour periods were binned by season. The statistical significance of differences between up-valley and down-valley flow conditions during different seasons were evaluated using the non-parametric Kruskal-Wallis and Mann-Whitney tests. The distribution ofdifferences in BC concentrations between up-valley and down-valley flows are quite similar yet statistically significant for all seasons, with higher down-valley concentrations (Figure 7a). However, because wind velocities were relatively higher during up-valley daytime flow and the durations of up-valley were modestly longer than those of down-valley flow, the corresponding up-valley fluxes of BC during daytime were markedly and significantly greater than down-valley fluxes during all seasons (Fig. 7b). These results suggest an oscillatory movement of polluted air within the valley, where polluted air masses are pushed up-valley during daytime and retreat a shorter distance during nighttime. These Ddifferences between up-valley andversus down-valley fluxes yielded significant net dailypositive up-valley fluxes of BC during all seasons (Fig. 7c). Because heating would have driven growth of the boundary layer and thus greater ventilation and dilution of pollutants during daytime relative to night, we infer that the calculated differences in up-valley versus down-valley fluxes correspond to lower limits for net BC fluxes.

Positive up-valley fluxes are consistent with an "alpine pumping" mechanism in the Himalayan valleys and thereby support the hypothesis that these valleys are important pathways for pollution transport. ~~If we assume that (1) the polluted boundary layer within the valley at Jomsom is 800 m deep (i.e., the approximate elevational difference between the two AWS sites at Jomsom), (2) BC within the polluted boundary layer is well mixed, and (3) wind velocities do not vary significantly with altitude through the polluted layer, the mass flux BC through a vertical plane across the valley can be estimated. Because .~~ ~~Supplementary Figure 2 shows that during daytime JSM_2 is well within the polluted haze layer during daytime/ upvalley flows and some BC is almost certainly transported above 800 m elevation where wind speed is about 5 m s^{-1} higher, thus this approach yields a conservative estimate. The long lifetime of particulate BC against deposition (several days to a week or more) coupled with turbulent flow within the valley supports the assumption that BC is well mixed. As noted previously, wind velocities measured at JSM_1 (2800 m) and JSM_2 (3700 m) were similar suggesting minimal variability through the lower 800 m depth of the valley. Extrapolation of the net daily BC flux per unit area to the cross-sectional plane of the valley at Jomsom (1.62 km^2) yields~~ In addition, we estimate substantial net daily mass transport~~fluxes amount~~ of BC ~~through the~~ up the valley during the pre-monsoon season~~: of~~ 1.05 kg day^{-1} (based on the average ~~daily~~ net daily flux) and 0.72 kg day^{-1} (based on the median ~~daily~~ net daily flux). While preliminary, these ~~Such~~ estimates provide the first ~~useful~~ semi-quantitative constraints on mass ~~fluxes~~ transport of BC from the IGP to the high Himalaya through deep valleys and, more generally, on the regional cycling of BC over southern Asia.

3.5 Evidence of regional transport episodes in valley concentration

Along with the regular diurnal and seasonal variability driven by local winds as described above, we also observed anomalous periods – lasting ~~when for~~ several days to more than a week – during ~~which~~ BC concentrations ~~of both BC and O_3~~ were significantly greater than the 90th percentile for corresponding annual averages (Table 3). ~~(Supplementary Table 3).~~ These extended periods of high BC ~~and O_3~~ at JSM_STA are evidence of large-scale transport from the IGP to the foothills in conjunction with local valley winds (Fig. 8). ~~We identified three common patterns in the BC profile at Jomsom during the transport episodes. For most~~ Most of the transport episodes were associated with ~~observational evidence from satellite imagery of emission sources within the region including haze over IGP, agricultural and biomass burning in Punjab regions of India and Pakistan, and forest fires in the foothills of the Himalaya in northern India or southern Nepal (Supplement Table 3). Pollutant source location could not be identified at times due to cloud cover. The 90th percentile for each year 2013, 2014~~

Formatted: Superscript

and 2015 were 1.53 µg m^{-3}, 1.60 µg m^{-3} and 1.47 µg m^{-3} respectively. The year 2015 only included January through July data. Analogous increment, above 90th percentile, in Elevated O_3 concentrations did not always accompany these long-duration periods of high occur when BC concentrations were above 90th percentile. Different atmospheric lifetimes, chemical reactivity, source location, and sinks of BC and O_3 all may contribute to have been responsible for these differences in BC and O_3 concentrations detected in the valley. Table 3 reports the number of days in which O_3 concentration was above 90th percentile within each episode.

We partitioned these episodes into three characteristic patterns based on the relative variability of BC. Pattern A was characterized as a fluctuating daily maximuma in BC with peaks that repeatedly exceeded the 90th percentile but with daily minima below the 90th percentile relatively lower minima (Fig. 8[Ia]). Pattern B was characterized by as regional transport periods when a steady buildup of BC concentration was seen over the period of the regional transport episode, with peak BC concentrations over the 90th percentile but without a relatively low daily minimum a but peak concentrations over the 90th percentile (Figure 8b). While Pattern C exhibited a combination of corresponded to the periods when the BC concentration exhibited both Ppatterns A and B during a single regional episode (Figure 8c). A total of 341 regional episodes were identified from January 2013 throughill Junely 2015, 47 50% of which were categorized as Ppattern A, 320% as Pattern B, and 210% as pPattern C. The wind speeds at Jomsom during these transport episodes exhibited diurnal variability similar to those during other periods (Fig. 8 [II]). We initiated the Hybrid Single-Particle Lagrangian Integrated Trajectory model (HYSPLIT), developed by NOAA's Air Resources Laboratory, from 300 m, 500 m and 1000 m for 72 hours runtime for each of the example episodes (Stein et al., 2015). HYSPLIT trajectories show that the transport of air mass from the above source regions during that period (Fig. 9).

During the regional transport period in November 2014 (Pattern A), average daily BC concentration was 1.29 µg m^{-3} which is over the 75th percentile (0.88 µg m^{-3}) of the BC concentration for the measurement duration. The maximum daily concentration during the period was 3.04 µg m^{-3}. However, the corresponding average O_3 was only 28.07 ppbv, slightly below the average (29.48 ppbv) for the entire data set (Figure 8 [Ia]). The diurnal wind pattern in the KGV was conserved during pattern A (Figure 8 [IIa]). The mean BC concentration during pattern B, one example of which occurred in May 2014, was 1.77 µg m^{-3} (Figure 8[Ib]). It was above the 90th percentile (1.49 µg m^{-3}) for entire measurement period while O_3 concentrations were at 49.71 ppbv, slightly below the 90th percentile (52.9 ppbv). The wind pattern in the KGV exhibited diurnal flow patterns but with longer period of up-

Formatted: Subscript
Formatted: Superscript
Formatted: Subscript
Formatted: Subscript
Formatted: Subscript
Formatted: Superscript
Formatted: Superscript

valley flows compared to pattern A (Fig. 8 [IIb]). One of the Pattern C- type of transport episodes was identified in May 2013, when the average concentration was well above the 90th percentile for both BC (2.09 µg m^{-3}) and O_3 (57.49 ppbv) (Fig. 8 [Ic]). Diurnal wind patterns were similar to those of pattern B with extended duration of up-valley flows (Fig. 8 [IIc]).The diurnal wind pattern in the KGV was conserved during the Pattern A example, but a longer period of up-valley flows occurred during the examples for Patterns B and C (Fig. 8).

We initiated the Hybrid Single-Particle Lagrangian Integrated Trajectory model (HYSPLIT), developed by NOAA's Air Resources Laboratory, from 300 m, 500 m and 1000 m for 72 hours runtime for each of the example episodes (Stein et al., 2015). The back trajectories were initiated at the mouth of the valley on the day when fire events were the most visible on MODIS imagery within each example episodes in Figure 8. The results though mostly qualitative show that regional episodes occurred when extensive haze or fire events were detected in the Indo-Gangetic plains (Supplementary Figure 2). The MODIS fire data and HYSPLIT back trajectories showed extensive haze and fire events during this period of regional transport (Figure 9). We infer that transport of BC emitted from agricultural burning and wildfires during this period contributed to the high concentration measured with the KGV.

The mean BC concentration during pattern B, one example of which occurred in May 2014, was 1.77 µg m^{-3} (Figure 8[Ib]). It was above the 90th percentile (1.49 µg m^{-3}) for entire measurement period while O_3 concentrations were at 49.71 ppbv, slightly below the 90th percentile (52.9 ppbv). The wind pattern in the KGV exhibited diurnal flow patterns but with longer period of up-valley flows compared to pattern A (Fig. 8 [IIb]). During this period MODIS imagery and HYSPLIT back trajectories revealed widespread burning in the Himalayan foothills and the Punjab region of India (Figure 9).

One of the Pattern C- type of transport episodes was identified in May 2013, when the average concentration was well above the 90th percentile for both BC (2.09 µg m^{-3}) and O_3 (57.49 ppbv) (Fig. 8 [Ic]). Diurnal wind patterns were similar to those of pattern B with extended duration of up-valley flows (Fig. 8 [IIc]). MODIS and HYSPLIT back trajectories revealed extensive agricultural burning in the Punjab region of India and the southern plains of Nepal during this period (Figure 9).

3.5 Pollution in the Higher Himalaya

Average BC concentrations in European cities including Barcelona, Lugano and London range between

~~1.7 to 1.9 μg m^{-3} (Reche et al., 2011). National Ambient Air Quality Standards (NAAQS) for the United States for O_3 is 70 ppbv (8-hour maximum average). During regional transport episodes, BC and O_3 levels in the remote site in Jomsom occasionally exceeded the above levels for both BC and O_3. BC and O_3 concentrations suggest that the extensive haze layer over the IGP during pre-monsoon along with increased fire activity in the IGP and Himalayan foothills results in an increased flux of pollutants into the Himalayan valleys (Fig. 7 and 8). The pollutants are transported by the local wind system, specifically the up-valley winds that are dominant throughout the day. However, larger synoptic patterns are responsible for transport of pollutants from regional sources to the Himalayan foothills and the entrance region of valleys like the KGV.~~

~~The results obtained at JSM_STA show similar seasonal pattern as NCO-P CNR (Bonasoni et al., 2010) with higher concentration of BC and O_3 in the pre-monsoon season and lowest during the monsoon. However, the magnitude of concentration differ for both BC and O_3 at the two sites (Table 1). Our results from JSM_STA found BC concentrations in the KGV are twice as high as those measured at NCO-P CNR during pre-monsoon season while O_3 concentration at NCO-P CNR were twice as high as JSM_STA. At JSM_STA during the post monsoon season, BC concentration are comparative to pre-monsoon season and 5 times higher than that at NCO-P CNR while O_3 concentrations remain higher at NCO-P CNR. The NCO-P CNR is at a higher elevation than Jomsom and can be affected by frequent stratospheric intrusions thus resulting in higher O_3 concentrations than that at Jomsom (Cristofanelli et al., 2010). Alternatively, BC is significantly higher in Jomsom for all seasons when compared to NCO-P CNR.~~

4. Conclusion

This study provides new in-situ observational evidence of the role of a major Himalayan valley as an important pathway for transporting air pollutants from the IGP to the higher Himalaya. We found that~~:~~

~~C~~ concentrations of BC and O_3 in the KGV exhibited systematic diurnal and seasonal variability. The diurnal pattern of BC concentrations during the pre- and post-monsoon seasons were modulated by the pulsed nature of up-valley and down-valley flows. Seasonally, pre-monsoon BC concentrations ~~of BC~~ were higher than in post-monsoon season.

We also found that ~~The~~ morning and afternoon peaks in the post~~-~~monsoon season were~~as~~ more pronounced than those of pre-monsoon season, likely due to the relatively lower wind speeds during post-monsoon.

~~When compared to a high elevation site, NCO-P CNR in the Himalaya, JSM_STA consistently showed higher BC concentrations for all seasons whereas the corresponding O_3 concentrations were higher at NCO-P CNR.~~

Significant positive up-valley fluxes of BC were measured during all seasons and preliminary flux estimates (which require a more robust estimate in future work) show the efficiency and magnitude of pollutant transport up the valley.~~.~~

During episodes of regional pollution over the IGP, relatively higher concentrations of BC and O_3 were also measured in the KGV.

The frequency and magnitude of pollution events highlighted in the paper need to be studied for a longer period in order to understand the associated interannual variability. ~~The flux measurement provided shows the efficiency of pollutant transport through the valley. However, further studies are required for a robust quantification of the fluxes.~~ ~~Further~~ In addition, future work should focus on ~~studies are needed to~~ understand~~ing~~ the vertical and horizontal distribution of particulate matter and ozone in the Himalayan region, and their impact~~s~~ on the radiative budget, the ASM and regional climate. ~~Investigations using sondes, LiDar and air-borne measurements could help characterize the stratification of the vertical air masses.~~

Acknowledgments

We would like to acknowledge our field assistant in Nepal, Buddhi Lamichhane who helped us in various stages of the study, as well as the logistic and administrative support and internet at the Jomsom station provided by Nepal Wireless. Financial support was provided by the National Aeronautics and Space Administration NNX12AC60G, and additional field support was provided by ICIMOD's Atmosphere Initiative. The authors are very thankful for comments from William Keene and Jennie Moody.

605

References

Andreae, M. O. and Crutzen, P. J.: Atmospheric Aerosols: Biogeochemical Sources and Role in Atmospheric Chemistry, Science, 1052-1058, 1997.

Auffhammer, M., Ramanathan, V. and Vincent, J. R.: Integrated model shows that atmospheric brown
610 clouds and greenhouse gases have reduced rice harvests in India, *PNAS* 10.1073/pnas.0609584104, 2006.

Bonasoni, P., Laj, P., Marinoni, A., Sprenger, M., Angelini, F., Ar- duini, J., Bonafe, U., Calzolari, F., Colombo, T., Decesari, S., Di Biagio, C., di Sarra, A. G., Evangelisti, F., Duchi, R., Facchini, M. C., Fuzzi, S., Gobbi, G. P., Maione, M., Panday, A., Roccato, F., Sellegri, K., Venzac, H., Verza, G. P.,
615 Villani, P., Vuillermoz, E., and Cristofanelli, P.: Atmospheric Brown Clouds in the Himalayas: first two years of continuous observations at the Nepal Climate Observatory-Pyramid (5079 m), *Atmos. Chem. Phys.*, 10, 7515–7531, doi:10.5194/acp-10-7515-2010, 2010.

Bond, T., Doherty, S., Fahey, D., Forster, P., Berntsen, T., DeAngelo, B., Flanner, M., Ghan, S., Kärcher, B., and Koch, D.: Bounding the role of black carbon in the climate system: A scientific
620 assessment, J. Geophys. Res.-Atmos., 118, 5380–5552, doi:10.1002/jgrd.50171, 2013.

Brun, J., Shrestha, P., Barros, A., P.: Mapping aerosol intrusion in Himalayan valleys using the Moderate Resolution Imaging Spectroradiometer (MODIS) and Cloud Aerosol Lidar and Infrared Pathfinder Satellite Observation (CALIPSO), *Atmos. Env*., 45 (2011) 6382-6392, 2011.

Cristofanelli, P., Bracci, A., Sprenger, M., Marinoni, A., Bonafè, U., Calzolari, F., Duchi, R., Laj, P.,
625 Pichon, J. M., Roccato, F., Venzac, H., Vuillermoz, E., and Bonasoni, P.: Tropospheric ozone variations at the Nepal Climate Observatory-Pyramid (Himalayas, 5079 m a.s.l.) and influence of deep stratospheric intrusion events, Atmos. Chem. Phys., 10, 6537–6549, doi:10.5194/acp-10-6537-2010, 2010.

Dey, S., and Di Girolamo, L.: A climatology of aerosol optical and microphysical properties over the Indian subcontinent from 9 yr (2000–2008) of Multiangle Imaging Spectroradiometer (MISR) data, *J. Geophys. Res.*, 115, D15204, doi:10.1029/2009JD013395, 2010.

Decesari, S., Facchini, M.C., Carbone, C., Giulianelli, L., Rinaldi, M., Finessi, E., Fuzzi, S., Marinoni, A., Cristofanelli, P., Duchi, R., Bonasoni, P., Vuillermoz, E., Cozic, J., Jaffrezo, J., L., Laj, P.: Chemical composition of PM_{10} and PM_1 at the high-altitude Himalayan station Nepal Climate Observatory-Pyramid (NCO-P) (5079 m a.s.l.), *Atmos. Chem. Phys.*, 10: 4583–4596, 2010.

DOTM-Vehicle data zonal wise till 2072 baishakh, Government of Nepal, Department of Transportation Management (http://www.dotm.gov.np/uploads/files/Vehicle-data-zonal-wise-till-2072-baishakh.pdf) accessed March 26th, 2016.

Dumka, U., C., Krishna Moorthy, K., Satheesh, S., K., Sagar, R., Pant, P.: Short-period modulations in aerosol optical depths over the central Himalayas: role of mesoscale processes, *J. Appl. Meteor. Climatol.*, doi: 10.1175/2007JAMC1638.1, 2008.

Dumka, U., C., Moorthy, K., K., Kumar, R., Hegde, P., Sagar, R., Pant, P., Singh, N., Babu, S.: Characteristics of aerosol black carbon mass concentration over the high altitude location in the central Himalayas from multi-year observations. *Atmos. Res.*, 96, 510-521 2010.

Egger, J., Bajracharya, S., Egger, U., Heinrich, R., Reuder, J., Shakya, P., Wendt, H., and Wirth, V.: Diurnal winds in the Himalayan Kali Gandaki valley. Part I: observations, *Mon. Weather Rev.*, 128, 1106-1122, 2000.

Egger, J., Bajracharya, S., Egger, U., Heinrich, R., Kolb, P., Lammlein, S., Mech, M., Reuder, J., Schaper, W., Shakya, P., Schween, J. and Wendt, H.: Diurnal winds in the Himalayan Kali Gandaki valley. Part III:remotely piloted aircraft soundings, *Mon. Weather Rev*., 130, 2042-2058, 2002.

Engling, G., and Galencser, A.: Atmospheric brown clouds: from local air pollution to climate change, *Elements*, 6, 223-228, 2010.

Fadnavis, S., Semeniuk, K., Pozzoli, L., Schultz, M. G., Ghude, S. D., Das, S., and Kakatkar, R.: Transport of aerosols into the UTLS and their impact on the Asian monsoon region as seen in a global model simulation, Atmos. Chem. Phys., 13, 8771–8786, 2013.

Fischer, E., Pszenny, A., Keene, W., Maben, J., Smith, A., Stohl, A., Talbot R.: Nitric acid phase partitioning and cycling in the New England coastal atmosphere, J. Geophys. Res., 111, D23S09,

doi:10.1029/2006JD007328, 2006.

Flanner, M. G., Zender, C. S. , Hess, P. G., Mahowald, N. M., Painter, T. H., Ramanathan, V., Rasch , P. J.: Springtime warming and reduced snow cover from carbonaceous particles, Atmos. Chem. Phys., 9 (7), 2481- 2497, doi: 10.5194/acp-9-2481-2009, 2009.

Gautam, R., Hsu, N., C., Tsay, S., C., Lau, K., M., Holben, B., Bell, S., Smirnov, A., Li, C., Hansell, R., Ji, Q., S. Payra, S., Aryal, D., Kayastha, R., K. M. Kim, K., M. : Accumulation of aerosols over the Indo-Gangetic plains and southern slopes of the Himalayas: distribution, properties and radiative effects during the 2009 pre-monsoon season, *Atmos. Chem. Phys.*, 11, 12841–12863, 2011

Gustafsson, O., Kruså, M., Zencak, Z., Sheesley, R., J., Granat, L., Engström,E., Praveen, P., S., Rao, P., S., P., Leck, C., Rodhe, H.: Brown Clouds over South Asia: Biomass or Fossil Fuel Combustion?, *Science*, 323, 495-498, 2009.

~~Hegde P., Pant, P., Naja, M., Dumka, U. C., and Sagar, R.: South Asian dust episode in June 2006: Aerosol observations in the central Himalayas, *Geophys. Res. Lett.*, 34, L23802, doi:10.1029/2007GL030692, 2007.~~

Henne, S., Furger, M., Nyeki, S., Steinbacher, M., Neininger, B., de Wekker, S.F.J, Dommen, J., Spichtinger, N., A. Stohl, A. and Prevót A. S. H.: Quantification of topographic venting of boundary layer air to the free troposphere, *Atmos. Chem. Phys.*, 4, 497–509, 2004.

~~Hindman, E. E. and Upadhyay, B. P.: Air pollution transport in the Himalayas of Nepal and Tibet during the 1995–1996 dry season, *Atmos. Environ.*, 36, 727–739, 2002.~~

Hyvärinen, A., P., Lihavainen, H., Komppula, M., Sharma, V., P., Kerminen, V., M., Panwar, T., S., Viisanen, Y.: Continuous measurements of optical properties of atmospheric aerosols in Mukteshwar, Northern India, *J. Geophys. Res.*, 114: D08207, doi: 10.1029/2008JD011489, 2009.

Hyvarinen, A., -P., Vakkari, V., Laakso, L., R. K. Hooda, R., K., Sharma, V., P., Panwar, T., S., Beukes, J., P., van Zyl, P., G., M. Josipovic, M., Garland, R. M., Andreae, M. O., Poschl, U., Petzold, A. : Correction for a measurement artifact of the Multi-Angle Absorption Photometer (MAAP) at high black carbon mass concentration levels, *Atmos. Meas. Tech.*, 6, 81–90, 2013

Jacobson, M., Z.: Strong radiative heating due to the mixing state of black carbon in atmospheric aerosols, *Nature*, 409, 695-697, 2001.

Janssen, Nicole A. H., Hoek, G., Simic-Lawson, M., Fischer, P., van Bree, L., Brink, H., Keuken, M., Atkinson, R. W., Anderson, H. R., Brunekreef, B., and Cassee, F. R.: Black carbon as an additional indicator of the adverse health effects of airborne particles compared with PM_{10} and $PM_{2.5}$, *Environ. health persp.* 119 (12), 1691-1698, 2011.

Kang, S., Xu, Y., You, Q., Flugel, W-A., Pepin, N. and Yao, T. review of Climate and cryospheric change in the Tibetan Plateau, *Environ. Res. Lett.* 5(1), 015101, 2010.

Kaufman, Y. J., Tanré, D., and Boucher, O.: A satellite view of aerosols in the climate system, *Nature*, 419, 215–223, 2002.

Koch, D., Schulz, M., Kinne, S., McNaughton, C., Spackman, J.R., Balkanski, Y., Bauer, S., Berntsen, T., Bond, T.C., Boucher, O., Chin, M., Clarke, A., De Luca, N., Dentener, F., Diehl, T., Dubovik, O., Easter, R., Farey, D.W., Feichter, J., Fillmore, D., Freitag, S., Ghan, S., Ginoux, P., Gong, S., Horowitz, L., Iversen, T., Kirkevåg, A., Klimont, Z., Kondo, Y., Krol, M., Liu, X., Miller, R., Montanaro, V., Moteki, N., Myhre, G., Penner, J.E., Perlwitz, J., Pitari, G., Reddy, S., Sahu, L., Sakamoto, H., Schuster, G., Schwarz, J.P., Seland Ø, Stier P., Takegawa, N., Takemura, T., Textor, C., van Aardenne, J.A., Zhao, Y.: Evaluation of black carbon esti- mations in global aerosol models. Atmospheric Chemistry and Physics 9, 9001e9026.Komppula, M., Lihavainen, H., A.-P. Hyvärinen,A., -P., Kerminen, V., –M., Panwar, T., S., Sharma, V., P., Viisanen, Y.: Physical properties of aerosol particles at a Himalayan background site in India, *J. Geophys. Res.*, 112, doi:10.1029/2008JD011007, 2009.

Kopacz, M., Mauzerall,D., L., Wang, J.,Leibensperger, E., M., Henze, D., K., and K. Singh, K.: Origin and radiative forcing of black carbon transported to the Himalayas and Tibetan Plateau, *Atmos. Chem. Phys.*, 11, 2837–2852, 2011.

Krupnick, A., J., Harrington, W., Ostro, B.: Ambient ozone and acute health effects: Evidence from daily data, *J. Environ. Econ. Manag.*, 18(1), 1-18, 1990.

Lau, K., M., Kim, M., K., Kim, K., M.: Asian summer monsoon anomalies induced by aerosol direct forcing: The role of the Tibetan Plateau, *Climate Dynamics*, 26, 855–864, 2006.

Lawrence, M. G. and Lelieveld, J.: Atmospheric pollutant outflow from southern Asia: a review, *Atmos. Chem. Phys.*, 10, 11017–11096, doi:10.5194/acp-10-11017-2010, 2010.

Lee K, Soon DH, Shugui H, Sungmin, Xiang Q, Jaiwen R, Yapping L, Rosmann KJRR, Barbante C, Bourton CF.: Atmospheric pollution of trace elements in the remote high-altitude atmosphere in

Central Asia as recorded in snow from Mt Qomolangma (Everest) of the Himalayas, *Sci. Tot. Environ.* 404, 171-181, 2008.

Lu, Z., Zhang, Q., and Streets, D., G.: Sulfur dioxide and primary carbonaceous aerosol emissions in China and India, 1996–2010, *Atmos. Chem. Phys.*, 11, 9839-9864, 2011.

~~Luthi, Z., L., Skerlak, B., Kim, S., W., Lauer, A., Mues, A., Rupakheti, M., and Kang, S.: Atmospheric brown clouds reach the Tibetan Plateau by crossing the Himalayas, *Atmos. Chem. Phys.*, 15, 11, 6007-6021, 2015.~~

Ma, J., Chen, Y., Wang, W., Yan, P., Liu, H.,Yang, S., Hu, Z., and Lelieveld, J.: Strong air pollution causes widespread haze-clouds over China, *J. Geophys. Res.*, 115, D18204, 2010.

Marinoni, A., Cristofanelli, P., Laj, P., Duchi., R., Calzolari, F., Decesari, S., Sellegri, K., Vuillermoz, E., Verza, P., Villani, P., Bonasoni, P. Aerosol mass and black carbon concentrations, a two year record at NCO-P (5079 m, Southern Himalayas), *Atmos., Chem. Phys.*, 10, 8551-8562, 2010.

Marinoni, A., Cristofanelli, P., Laj, P., Duchi., R., Putero, D., Calzolari, F., Landi., T., C., Vuillermoz, E., Maione, M., Bonasoni, P.: High black carbon and ozone concentrations during pollution transport in the Himalayas: Five years of continuous observations at NCO-P global GAW station, *J. Environ. Sci.*, 25(8) 1618–1625, 2013.

Menon, S., Hansen, J., Nazarenko, L. and Yunfeng, L.: Climate Effects of Black Carbon Aerosols in Aerosols in China and India, *Science*, 297, 2250-2253, 2002.

Pant, P., Hegde, P., Dumka, U., C., Sagar, R., Satheesh, S., K., Krishna Moorthy, K., Saha, A., Srivastava, M., K.: Aerosol characteristics at high-altitude location in central Himalayas: optical properties and radiatuve forcing, *J. Geophys. Res.*, doi:10.1029/2005JD006768, 2006.

Piketh, S. J., Annegarn, H., J., and Tyson, P., D.: Lower tropospheric aerosol loadings over South Africa: The relative contribution of aeolian dust, industrial emissions, and biomass burning, *J. Geophys. Res.*, 104(D1), 1597–1607, 1999.

Qian, Y., Flanner, M. G., Leung, L. R., and Wang, W.: Sensitivity studies on the impacts of Tibetan Plateau snowpack pollution on the Asian hydrological cycle and monsoon climate, At- mos. Chem. Phys., 11, 1929–1948, doi:10.5194/acp-11-1929- 2011, 2011.

Raatikainen, T., Hyvärinen, A.-P., Hatakka, J., Panwar, T., S., Hooda, R., K., Sharma, V., P.,

Formatted: Space After: 8 pt

Lihavainen, H.: The effect of boundary layer dynamics on aerosol properties at the Indo-Gangetic plains and at the foothills of the Himalayas, *Atmos. Env.*, 89, 548-555, 2014.

Raatikainen, T., Brus, D., Hooda, R., K., Hyvärinen, A.-P., Asmi, E., Sharma, V., P., Arola, A., Lihavainen, H.: Size-selected black carbon mass distributions and mixing state in polluted and clean environments of northern India, *Atmos. Chem. Phys.* 17, 371-383, 2017.

Ram, K., Sarin, M., M. and Hegde, P.: Long-term record of aerosol optical properties and chemical composition from a high-altitude site (Manora Peak) in central Himalaya, *Atmos. Chem. Phys.*, 10: 11791–11803, 2010.

Ramanathan, V., and Carmichael, G.: Global and regional climate changes due to black carbon, *Nat. Geosci.*, 1(4), 221–227, 2008.

Ramanathan, V., Chung, C., Kim, D., Bettge, T., Buja, L., Kiehl, J., T., Washington, W., M., Fu, Q., Sikka, D., R., and Wild, M.: Atmospheric brown clouds: Impacts on South Asian climate and hydrological cycle, *PNAS*, 102(15), 5326-5333, 2005.

Ramanathan, V. and Crutzen, P. J.: New Directions: Atmospheric Brown "Clouds", Atmos. Env., 37, 4033-4035, 2003.

Ramanathan, V., Ramana, V., M., Roberts, G., Kim, D., Corrigan, C., Chung, C., Winker, D.: Warming trends in Asia amplified by brown cloud solar absorption, *Nature*, 448(2), 575-578, 2007a.

Ramanathan, V., Li, F., Ramana, M.V., Praveen, P.S., Kim, D., Corrigan, C.E., Nguyen, H., Stone, E.A., Schauer, J.J., Carmichael, G.R., Adhikary, B., Yoon, S.C.: Atmospheric Brown Clouds: Hemispherical and Regional Variations in Long-Range Transport, Absorption, and Radiative Forcing, *J. Geophys. Res.*, 112, D22821, 2007b.

Reche, C., Querol, X., Alastuey, A., Viana, M., Pey, J., Moreno, T., Rodríguez, S., González, Y., Fernández-Camacho, R., De La Campa, A. M, Sálnchez,De La Rosa, J., Dall'Osto, M., Prévôt, A. S H, Hueglin, C., Harrison, R. M., Quincey, P.: New considerations for PM, Black Carbon and particle number concentration for air quality monitoring across different European cities, *Atmos. Chem. Phys.*, 11, 6207–6227, 2011.

Reddy, M.S. and Venkataraman, C.: Inventory of Aerosol and Sulphur Dioxide Emissions from India: II – Biomass Combustion, Atmos. Envir., 36 (4), 699-712, 2002.

Reiter, E. R., and Tang, M.: Plateau effects on diurnal circulation patterns. *Mon. Wea. Rev.*, 112, 638–651, 1984.

Sander, R., Keene, W. C., Pszenny, A. A. P., Arimoto, R., Ayers, G. P., Baboukas, V., Chainey, J. M. Crutzen, P. J., Duce, R. A., Hönninger, G., Huebert, B. J., Maenhaut, W., Mihalopoulos, N., Turekian, V. C., van Dingenen, R.: Inorganic bromine in the marine boundary layer: A critical review, Atmos. Chem. Phys, 3, 1301-1336, 2003.

Sarangi, T., Naja, M., Ohja, N., Kumar, R., Lal, S., Venkataramani, S., Kumar, A., Sagar, R., Chandola, H., C.: First simultaneous measurements of ozone, CO and NO_y at a high-altitude regional representative site in the central Himalayas, *JGR*, 119(3), 1592-1611, 2014).

Singh R. P., Dey, S., Tripathi, S. N., Tare, V., and Holben, B.: Variability of aerosol parameters over Kanpur, northern India, *J. Geophys. Res.*, 109, D23206, doi:10.1029/2004JD004966, 2004.

Sreekanth, V., Niranjan, K., Madhavan, B. L.: Radiative forcing of Black Carbon over Eastern India, *Geophys. Res. Lett.*, 34(L17818), doi: 10.1029/2007GL030377, 2007.

Srivastava, A., K., Singh, S., Pant, P. and Dumka, U., C. : Characteristics of black carbon over Delhi and Manora peak - A comparative study, *Atmos. Sci. Lett.*,13: 223–230, 2012.

Stein, A.F., Draxler, R.R, Rolph, G.D., Stunder, B.J.B., Cohen, M.D., and Ngan, F., (2015). NOAA's HYSPLIT atmospheric transport and dispersion modeling system, Bull. Amer. Meteor. Soc., 96, 2059-2077, http://dx.doi.org/10.1175/BAMS-D-14-00110.1, 2015.

Steinacker, R.: Area–height distribution of a valley and its relation to the valley wind, Beitr. Phys. Atmos., 57, 64–71, 1984.

Streets, D. G., Bond, T. C., Carmichael, G. R., Fernandes, S. D., Fu, Q., He, D., Klimont, Z., Nelson, S. M., Tsai, N. Y., Wang, M. Q., Woo, J. H., and Yarber, K. F.: An inventory of gaseous and primary aerosol emissions in Asia in the year 2000, J. Geophys. Res.-Atmos., 108, 8809, doi:10.1029/2002JD003093, 2003.

The Royal Society, 2008. Ground-level ozone in the 21st century: future trends, impacts and policy implications. Science policy report 15/08. The Royal Society, London.

Tripathi, S. N., Dey, S., Tare, V., Satheesh, S. K.: Aerosol black carbon radiative forcing at an industrial city in northern India. Geophys. Res. Lett. 32 (L08802). doi:10.1029/2005GL022515, 2005.

Tripathi, S. N., Srivastava, A. K., Dey, S., Satheesh, S. K., Moorthy, K. K.: The vertical profile of atmospheric heating rate of black carbon aerosols at Kanpur in northern India. Atmos. Env.41: 6909–6915, 2007.

Ueno, K., Toyotsu, K., Bertolani, L., and Tartari, G.: Stepwise onset of Monsoon Weather Observed in the Nepal Himalayas, Mon. Weather Rev., 136(7), 2507–2522, 2008.

Vasilyev, O. B., Contreras, A., L., Velazquez, A., M., Fabi, R., P., Ivlev, L., S., Kovalenko, A., P., Vasilyev, A., V., Jukov, V., M., and Welch, R., M.: Spectral optical properties of the polluted atmosphere of Mexico City (spring-summer 1992), *J. Geophys. Res.*, 100(D12), 26027–26044, 1995.

Weissmann, M., Braun, A. F. J., Gantner, A., L., Mayr, A., G., J.,Rahm, A., S., Reitebuch, A., O. :The Alpine Mountain–Plain Circulation: Airborne Doppler Lidar Measurements and Numerical Simulations, *Mon. Weather Rev.*, 133,(11), 3095-3109, 2005.

Whiteman, C. D., and Bian X.: Use of radar profiler data to investigate large-scale thermally driven flows into the Rocky Mountains, *Proc. Fourth Int. Symp. on Tropospheric Profiling: Needs and Technologies*, Snowmass, CO, 1998.

Xu, C., Ma, Y. M., You, C., and Zhu, Z. K.: The regional distribution characteristics of aerosol optical depth over the Tibetan Plateau, *Atmos. Chem. Phys*., 15, 12065–12078, 2015.

Yasunari, T. J., Bonasoni, P., Laj, P., Fujita, K., Vuillermoz, E., Marinoni, A., Cristofanelli, P., Duchi, R., Tartari, G., and Lau, K.-M.: Estimated impact of black carbon deposition during pre- monsoon season from Nepal Climate Observatory - Pyramid data and snow albedo changes over Himalayan glaciers, Atmos. Chem. Phys., 10, 6603–6615, doi:10.5194/acp-10-6603-2010, 2010.

Zangl, G., Egger, J., and Wirth, V.: Diurnal Winds in the Himalayan Kali Gandaki Valley. Part II: Modeling, *Mon. Weather Rev*., 129, 1062-1080, 2000.

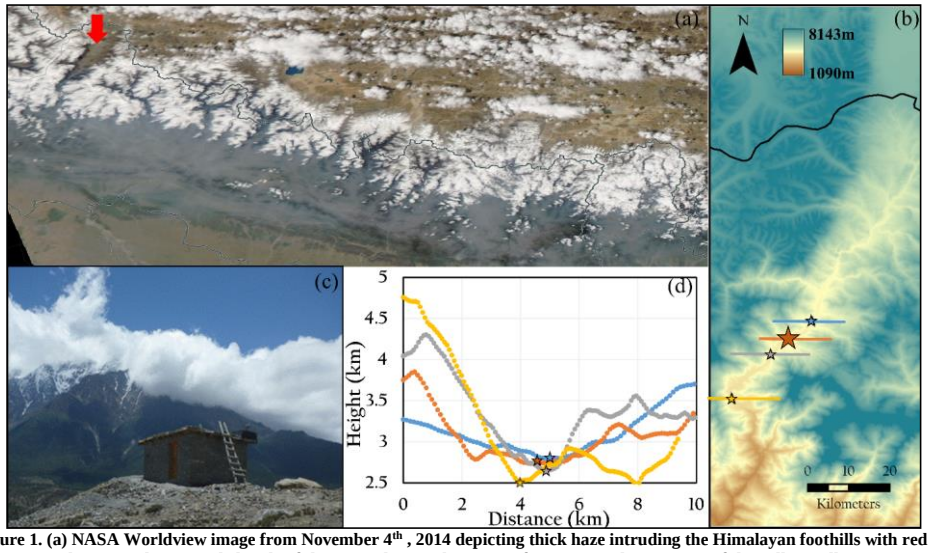

Figure 1. (a) NASA Worldview image from November 4th , 2014 depicting thick haze intruding the Himalayan foothills with red arrow over the KGV. (b) Expanded scale of the KGV showing locations of LET near the entrance of the valley (yellow star); MPH in the core region (gray star); the JSM_STA sampling station for BC and O_3 and the two associated AWS sites (JSM_1 and JSM_2) in the core region (orange star); and EKL near the exit (blue star). (c) The atmospheric observatory at Jomsom (JSM_STA). (d) Cross-sectional elevation profile at the indicated locations.

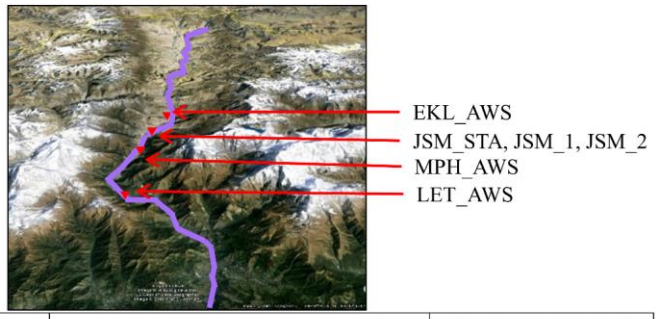

Station	Location	Elevation	Instrument(parameters measured)	Measurement period
JSM_STA	28.87N, 83.73E	2850m	Thermo BC MAAP–Model 5012 (Black carbon)	Jan 2013 – July 2015
			2B Tech Ozone instrument–Model 205 (Ozone)	Jan 2013 – July 2015
JSM_1	28.87N, 83.73E	2800m	DAVIS–Model Vantage Pro 2 (WD, WS, T, RH, DP)	Mar – May 2015
JSM_2	28.87N, 83.73E	3700m	NexSens–Model Vaisala WXT520 (WD, WS, T, RH, DP, Precip, Solar rad)	Jan 2013 – July 2015
LET_AWS	28.93N, 83.35E	2500m	Nexsens–ModelVaisala WXT520 (WD, WS, T, RH, DP, Precip, Solar rad)	Mar – May 2015
MPH_AWS	28.44N, 83.41E	2665m	HOBO–Model AWS U–30 (WD, WS, T)	Mar – May 2015
EKL_AWS	28.49N, 83.46E	2804m	NexSens–ModelVaisala WXT520 (WD, WS, T, RH, DP, Precip, Solar rad)	Mar – May 2015

Figure 2. The valley floor of KGV is shown in purple along with details pertaining to measurement sites, the installed instruments and measurement period.

855

860

Table 1. Data timeline for JSM_2 AWS, BC and O_3 measurements in Jomsom. Green indicates complete data, blue is with few data points missing, yellow is more than 15 days data, orange is less than 15 days and blank is no data.

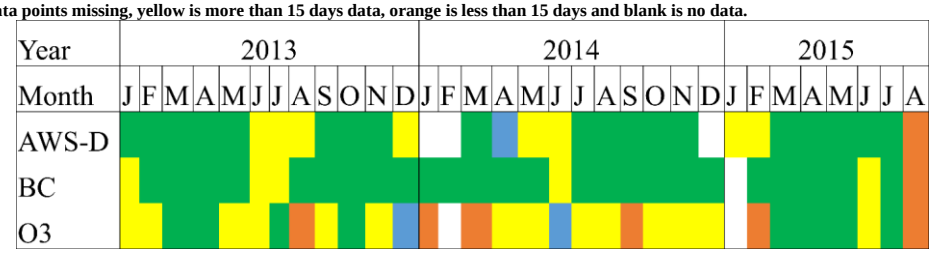

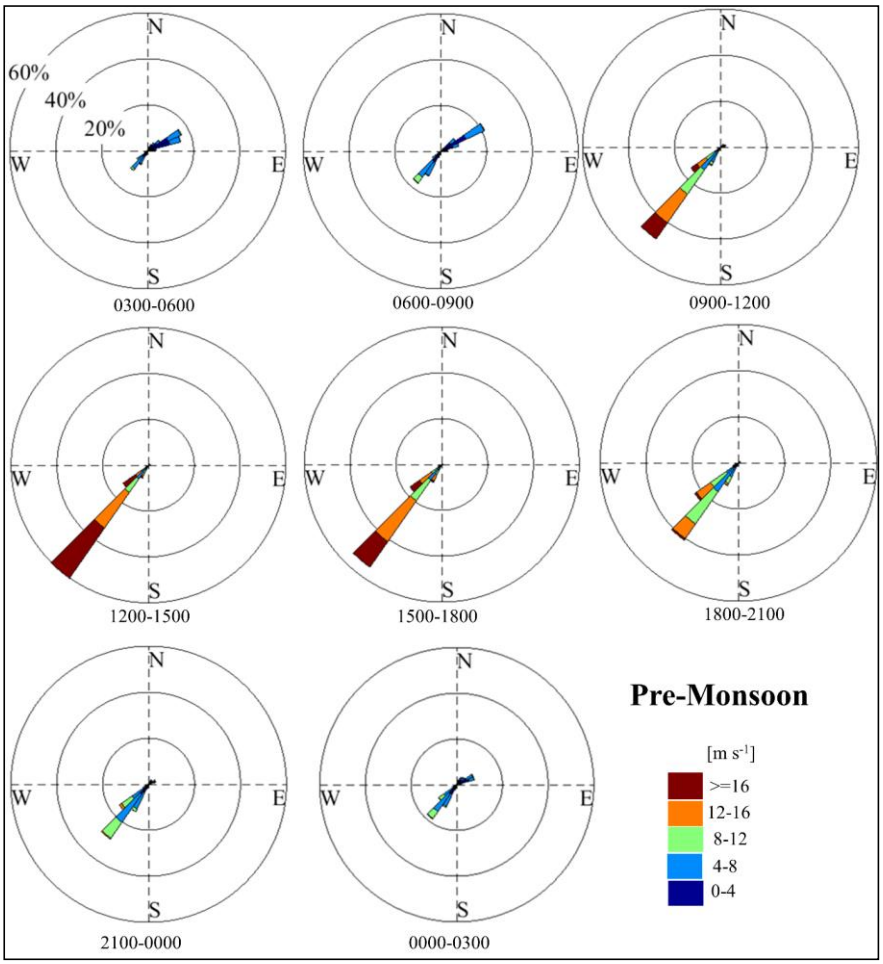

Figure 3a. Wind rose for pre-monsoon season – binned into 3-hour increments depiciting diurnal evolution in wind speed and direction at JSM_2.

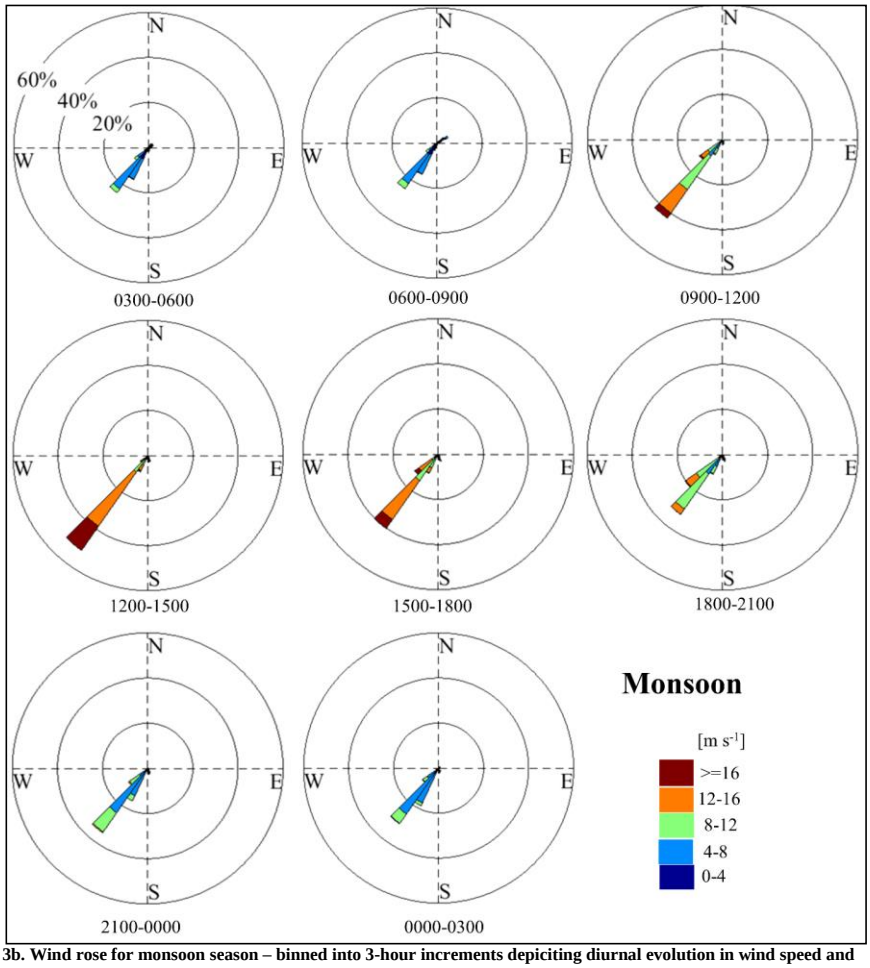

Figure 3b. Wind rose for monsoon season – binned into 3-hour increments depiciting diurnal evolution in wind speed and direction at JSM_2.

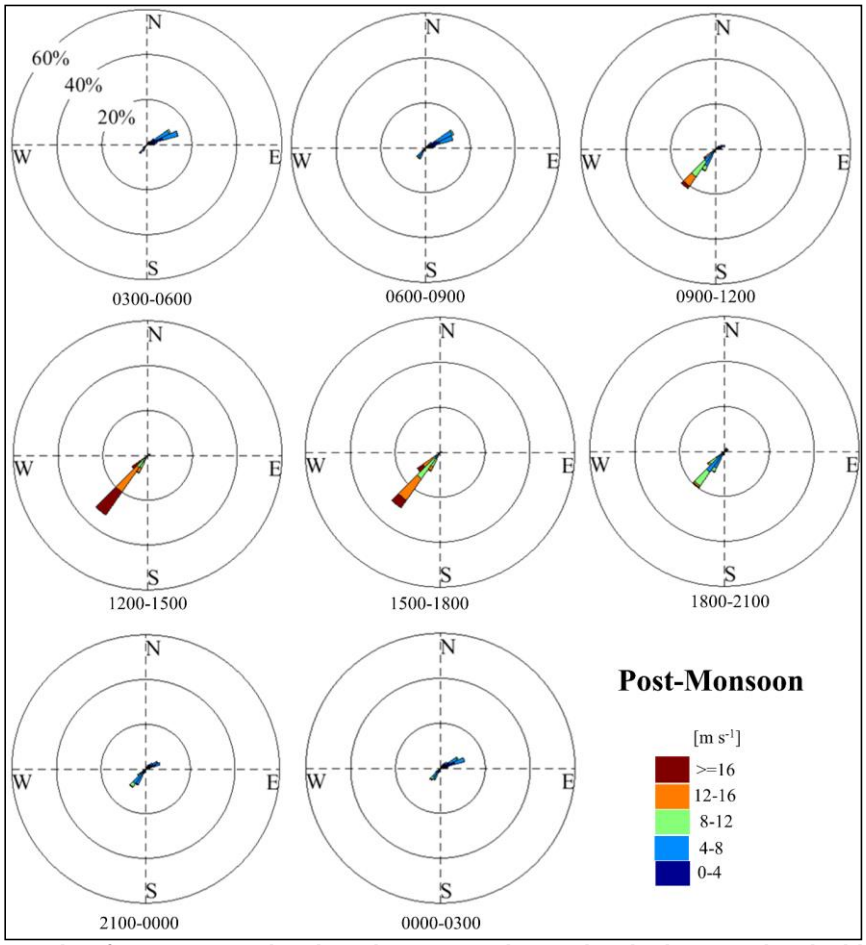

900 **Figure 3c. Wind rose for monsoon season – binned into 3-hour increments depiciting diurnal evolution in wind speed and direction at JSM_2.**

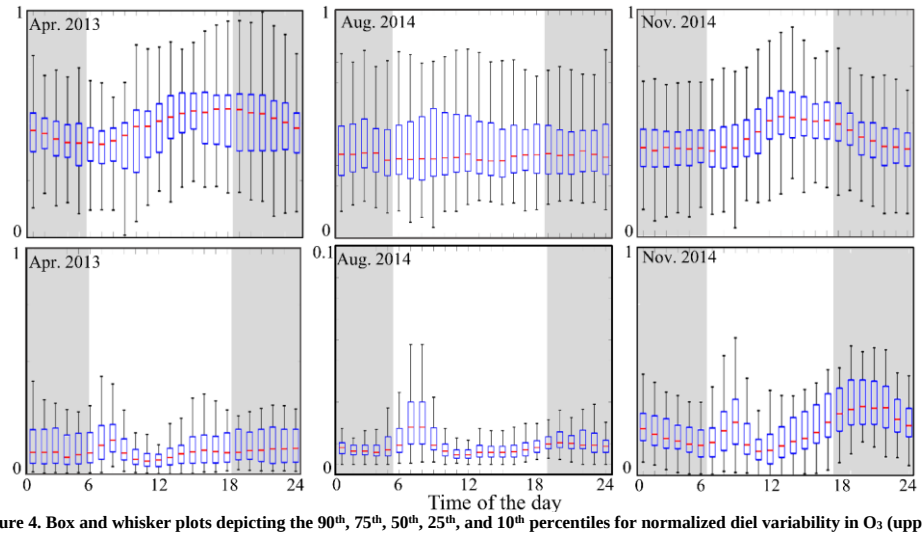

Figure 4. Box and whisker plots depicting the 90th, 75th, 50th, 25th, and 10th percentiles for normalized diel variability in O_3 (upper panels) and BC (lower panels) at JSM_STA during April 2013 (pre-monsoon), August 2014 (monsoon), and November 2014 (post-monsoon). Scale for August 2014 is from 0 to 0.1.

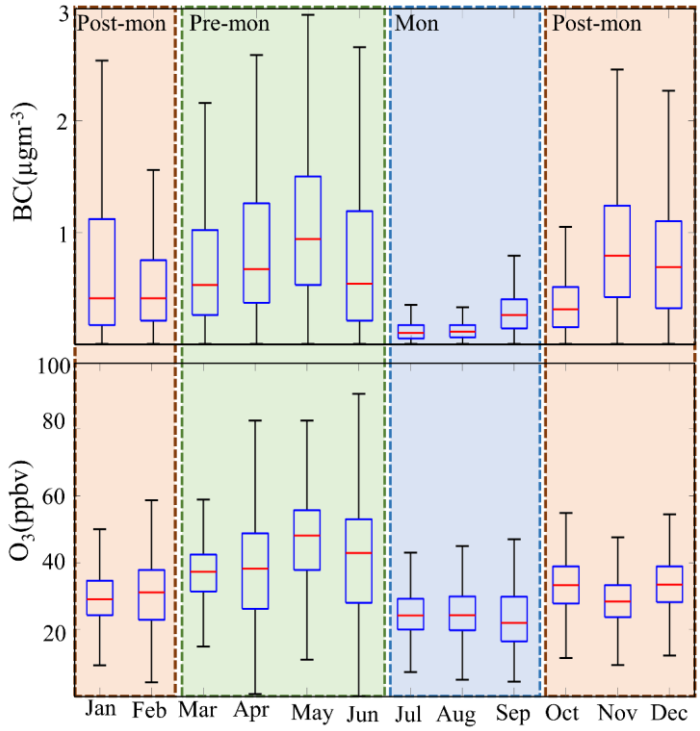

Figure 5. Box and whisker plots depicting the 90th, 75th, 50th, 25th, and 10th percentiles for monthly concentrations of BC (upper panel) and O3 (lower panel) between January 2013 and August 2015 at JSM_STA. Orange shaded areas indicate the post-monsoon season (Post-mon), green shaded area indicates the pre-monsoon (Pre-mon) and blue are indicates the monsoon (Mon) season.

Table 2. Comparison of BC and O_3 concentrations (mean ±standard deviation) between high elevation Himalayan site NCO-P CNR and JSM_1.

Sites	Altitude (m)	Co-ordinates	Season	BC (μg m^{-3})	O_3 (ppb)
NCO-P CNR (Bonasoni et al., 2010)	5079	27.95° N, 86.81° E	Pre-monsoon	0.317 (±0.34)	60.9 (±8.4)
			Monsoon	0.049 (±0.06)	38.9 (±9.6)
			Post-monsoon	0.135 (±0.08)	46.3 (±5.0)
JSM_1	2800	28.87° N, 83.73° E	Pre-monsoon	0.891 (±0.45)	39.5 (±8.23)
			Monsoon	0.207 (±0.24)	25.1 (±6.48)
			Post-monsoon	0.714 (±0.42)	31.4 (±4.5)

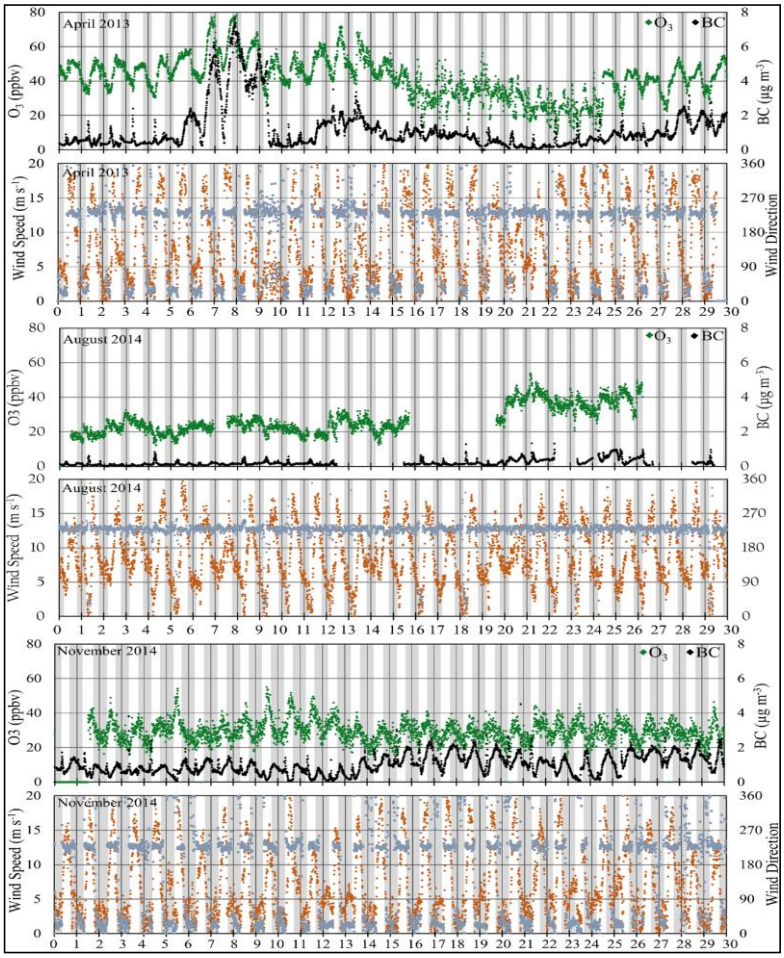

Figure 6. Variation in O_3, BC, and associated wind speed and direction at JSM_STA during (a) April 2013 (pre-monsoon), (b) July 2015 (monsoon), and (c) November 2014 (post monsoon). The grey shaded area denotes night.

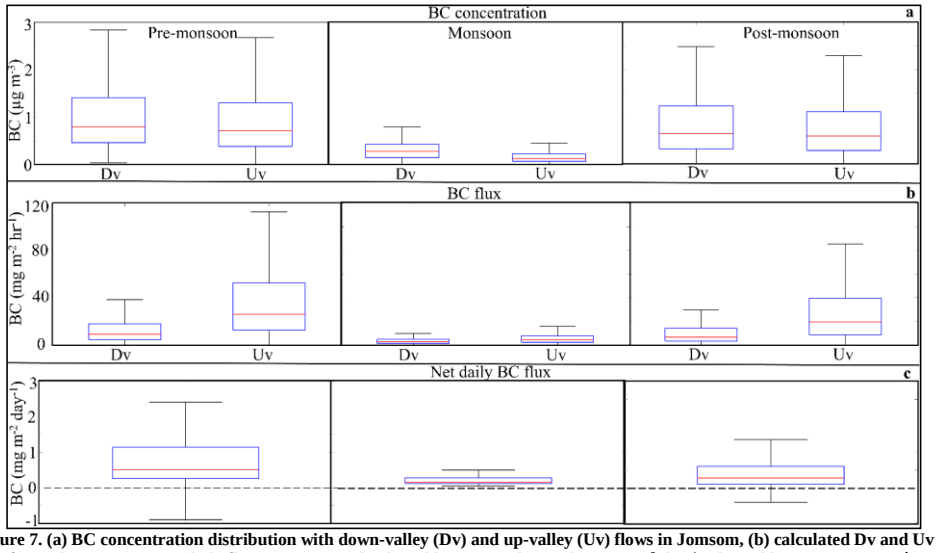

Figure 7. (a) BC concentration distribution with down-valley (Dv) and up-valley (Uv) flows in Jomsom, (b) calculated Dv and Uv flux for each season, (c) Net daily flux per season. The dotted line is panel c marks 0 mg m^{-2} day^{-1}. The red line represents 50th percentile, the edge of the box 25th and 75th percentile while the whiskers show maximum and minimum values.

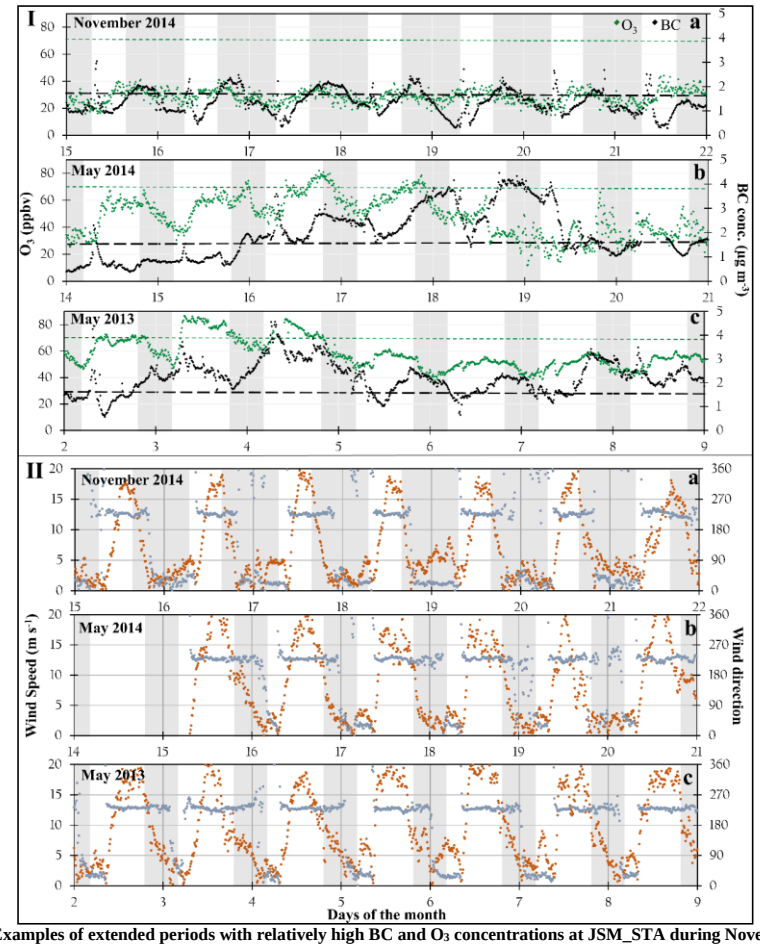

970 **Figure 8. (I) Examples of extended periods with relatively high BC and O_3 concentrations at JSM_STA during November 2014 (Pattern A) and May 2014 (Pattern B) and May 2013 (Pattern C). The dashed black and greeen lines depict two-year averages for BC and O_3, respectively. (II) Corresponding wind direction and wind speed during the high BC and O_3 episodes. The orange dots represent wind speed, and the blue dots represent wind direction.**

975 **Table 3. List of enhanced BC episodes observed at JSM_STA and the concurring regional sources from MODIS (* Data is from January-July; $^{+}$ Incomplete O_3 data)**

2013 (90th percentile : BC = 1.53 µg m^{-3} and O_3 = 49.5 ppbv)			
Month	**Episode Length**	**Episode type**	**Days with O_3 mixing ratio above 90th percentile**
Jan	6th – 15th	C	1
	28th – 31st	C	1+
Feb	Jan 28th – Feb 2nd	C	1+
Mar	1st – 3rd	A	0
	6th – 9th	A	0
	11th – 13th	B	0
	18th – 27th	B	4
Apr	6th – 10th	B	5
	12th – 14th	B	3
	27th – 30th	A	4
May	3rd – 11th	B	9
Oct	28th – 30th	A	No data
Nov	1st – 5th	A	No data
	23rd – 30th	A	0+
Dec	17th – 24th	C	0+
2014 (90th percentile: BC = 1.60 µg m^{-3} and O_3 = 56.8 ppbv)			
Month	**Episode Length**	**Episode type**	**Days with O_3 mixing ratio above 90th percentile**
Jan	13th – 15th	A	No data
Feb	Jan 31st – Feb 1st	A	No data
Mar	14th – 16th	A	No data
Apr	5th – 8th	B	2
	10th – 30th	C	15+
May	Apr 10th – May 1st	C	15+
	8th – 13th	B	6
	17th – 23rd	C	5+
Jun	5th – 8th	B	3
	10th – 17th	B	8
Nov	15th – 30th	A	0
Dec	Nov 15th – Dec 8th	A	0
2015 (90th percentile: BC = 1.47 µg m^{-3} and O_3 = 49.7 ppbv)			

Month	Episode Length	Episode type	Days with O_3 mixing ratio above 90th percentile
Jan	15th – 17th	A	No data
	21st – 25th	A	No data
Feb	21st – 26th	A	No data
May	6th – 9th	A	0^{+}
	18th – 26th	A	8
	29th – 31st	B	3
Jun	6th – 12th	B	7